Available online at www.sciencedirect.com
ScienceDirect
Global and Planetary Change 55 (2007) 90–108
GLOBAL AND PLANETARY CHANGE
www.elsevier.com/locate/gloplacha

Return to Coalsack Bluff and the Permian–Triassic boundary in Antarctica

Gregory J. Retallack [a,b,*], Tara Greaver [b], A. Hope Jahren [b]

[a] Department of Geological Sciences, University of Oregon, Eugene, Oregon 97403, USA
[b] Department of Earth and Planetary Sciences, Johns Hopkins University, Baltimore, Maryland 21218, USA

Received 2 July 2005; accepted 30 June 2006
Available online 20 September 2006

Abstract

Coalsack Bluff was the first discovery site in Antarctica for the latest Permian to earliest Triassic reptile *Lystrosaurus*. This together with discovery of Permian *Glossopteris* leaves during the heroic age of Antarctic exploration, indicated not only that Antarctica was part of Gondwanaland, but also that Antarctic rocks recorded faunas from the greatest of all mass extinctions at the Permian–Triassic boundary. Pinpointing the exact stratigraphic level of this life crisis has recently become possible using $\delta^{13}C$ values in terrestrial organic matter. Multiple, short-lived events of ^{13}C depletion may reflect carbon cycle crises, with the isotopic change a measure of terrestrial and atmospheric disequilibrium. Additional evidence for ecosystem reorganization came from changes in paleosol types and their root traces. Such studies previously completed at the Antarctic localities of Graphite Peak, Mount Crean, Portal Mountain, Shapeless Mountain and Allan Hills, are here extended to Coalsack Bluff. Carbon isotopic values in Permian rocks at Coalsack Bluff average −23.08±0.25‰, but begin to decline within the last coal with leaves (*Glossopteris*), roots (*Vertebraria*) and permineralized stumps (*Araucarioxylon*) of glossopterids. The low point in ä^{13}C values is −27.19‰ at 5.6 m above the last coal, which is capped by unusually abundant pyrite, and a claystone breccia with common clasts of redeposited clayey soils. Above this are massive quartz-rich sandstones of braided streams, considered a geomorphic response to deforestation and soil erosion following the mass extinction. Distinctive berthierine-bearing paleosols (Dolores pedotype) within these sandstones have unoxidized iron taken as evidence of severe groundwater hypoxia. Other paleosols at this stratigraphic level are like those in other Early Triassic rocks of Antarctica, which indicate unusually warm and humid conditions for such high paleolatitude lowlands. Waterlogging is also indicated by newly discovered kinds of paleosol (Ernest pedotype) with groundwater calcretes. The lack of peat accumulation in such waterlogged lowlands, berthierine in paleosols and large negative carbon isotopic shift at Coalsack Bluff support the idea of atmospheric pollution with methane from submarine and permafrost clathrates as a cause for the Permian–Triassic mass extinction. Hypoxic soils would have killed lowland plants by preventing root respiration and hypoxic air would have challenged vertebrates with pulmonary edema. Causes for catastrophic methane release remain unclear. Flood basalt eruptions, dolerite intrusions into coal measures, submarine landslides, tectonic faulting, and bolide impact suggested for episodes of methane release at other times are also plausible for the Permian–Triassic boundary.

Keywords: *Lystrosaurus*; *Glossopteris*; Permian; Triassic; mass extinction; Antarctica

* Corresponding author. Department of Geological Sciences, University of Oregon, Eugene, Oregon 97403, USA.
E-mail address: gregr@darkwing.uoregon.edu (G.J. Retallack).

0921-8181/$ - see front matter
doi:10.1016/j.gloplacha.2006.06.017

1. Introduction

Could there be greater evidence of dedication to scientific exploration than the 35 lb of *Glossopteris* fossils manhauled by Robert Falconer Scott's party to their fatal last camp on the Antarctica's Beardmore Glacier in 1913? Fossil wood, probably also from the Permian Buckley Formation in moraines of the Beardmore Glacier near Buckley Island at 85° S (Fig. 1), had been collected in 1909 by Ernest Shackleton's party. When British paleobotanist Albert Seward (1914) described these hard-won fossils it was clear that Permian–Triassic rocks were present in Antarctica. The likelihood of informative Permian–Triassic boundary sequences seemed remote until discovery by James A. Jensen on December 4, 1969 of the South African earliest Triassic therapsid *Lystrosaurus murrayi* on the slopes of Coalsack Bluff in the central Transantarctic Mountains (Fig. 2). A team of experienced bone-hunters including Edwin H. Colbert, William J. Breed and Jon S. Powell, had been sent to Antarctica following Peter Barrett's 1967 discovery of labyrinthodont bone scrap at Graphite Peak (Barrett et al., 1968), where eventually further specimens of *Lystrosaurus* and other early Triassic vertebrates were found (Colbert, 1974, 1983). Other central Transantarctic Mountain localities also yielded fossil vertebrates of the earliest Triassic *Lystrosaurus* zone (Fig. 1): Halfmoon Bluff, Collinson Ridge, Shenk Peak, Thrinaxodon Col (Colbert, 1983; Hammer, 1990). Additional vertebrates of the late Early Triassic *Cynognathus* zone have been found in Gordon Valley (Hammer, 1995), as well as earliest Jurassic dinosaurs on nearby Mt Kirkpatrick (Hammer and Hickerson, 1994). Discovery of Late Permian pollen (Tasch, 1978; Farabee et al., 1991), glossopterid reproductive structures (Schopf, 1976) and permineralized peats (Taylor et al., 1992; McManus et al., 2002) also encouraged the view that Antarctic sections might reveal details of the Permian–Triassic boundary, despite stratigraphic studies postulating a long disconformity at the boundary in Victoria Land (Isbell and Cuneo, 1996). The discovery in Austrian (Holser et al., 1989) and Chinese marine sequences (Xu and Yan, 1993) that the Permian–Triassic boundary could be recognized by a marked carbon isotopic ($\delta^{13}C$) depletion was then applied to non-marine rocks of Australia (Morante, 1996) and Antarctica (Krull and Retallack, 2000). Antarctic Permian–Triassic fluvial sediments not only formed at high southern paleolatitudes, but were well inland within the Gondwana supercontinent (Collinson et al., 1994), remote from paleotropical marine stratotype sections for the Permian–Triassic boundary in China (Jin et al., 2000). With the aid of carbon isotopic chemostratigraphy and renewed fossil plant collecting, the Permian–Triassic life crisis in Antarctica was found to be a marked extinction of paleosol pedotypes (Retallack and Krull, 1999). With new techniques of carbon isotope chemostratigraphy and new understanding of Antarctic paleosols, we returned to Coalsack Bluff, which remains an important and informative section for understanding the greatest of all mass extinctions at the Permian–Triassic boundary.

2. Materials and methods

Our expedition to Coalsack Bluff in December 2003 remeasured the section in the southwestern ridge (Fig. 3), using the method of eyeheights and a Brunton compass as a leveling device. The sequence dips at 29° to the west into the slope, and eyeheights were trigonometrically corrected for this dip. This remains the most informative section of the Permian–Triassic boundary on Coalsack Bluff, because it is well exposed (Fig. 1). The section is short because of Jurassic dikes above and below. Fossil plant and bone collections were made, and the location of old fossil quarries noted. Paleosols were classified using the pedotype classification outlined by Retallack and Krull, 1999 for other central Transantarctic sections. Color is from a Munsell color chart. Field testing for carbonate with dilute HCl revealed calcareous paleosols of a type not previously seen in Antarctica, and here designated the Ernest pedotype. This paleosol and the disctinctive Permian–Triassic boundary beds were studied by point counting petrographic thin sections in the Oregon laboratory of Retallack in order to quantify mineral and grain size variation. Unweathered samples of all carbonaceous lithologies were collected for bulk carbon isotopic determinations. In the Baltimore laboratory of Jahren these samples were macerated in HF and HCl, and rinsed. Organic carbon residues were prepared for stable isotope analysis by combustion in sealed tubes containing Cu, CuO, and Ag (Minagawa et al., 1984). Released CO_2 was purified cryogenically, and collected for $^{13}C/^{12}C$ measurement on an Isoprime Stable Isotope Ratio Mass Spectrometer, with all isotope values reported in permil (‰) relative to VPDB (Vienna Pee Dee Belemnite). There is no clear correlation between isotopic value and carbon abundance in the sample (Fig. 3). Nor is their any clear perturbation of carbon isotopic composition or carbon abundance with proximity to dolerite dikes at the top and bottom of the section, supporting the findings of Horner and Krissek (1991) that contact metamorphism of organic matter by these relatively anhydrous intrusions was spatially limited. Antarctic Permian coals are thermally

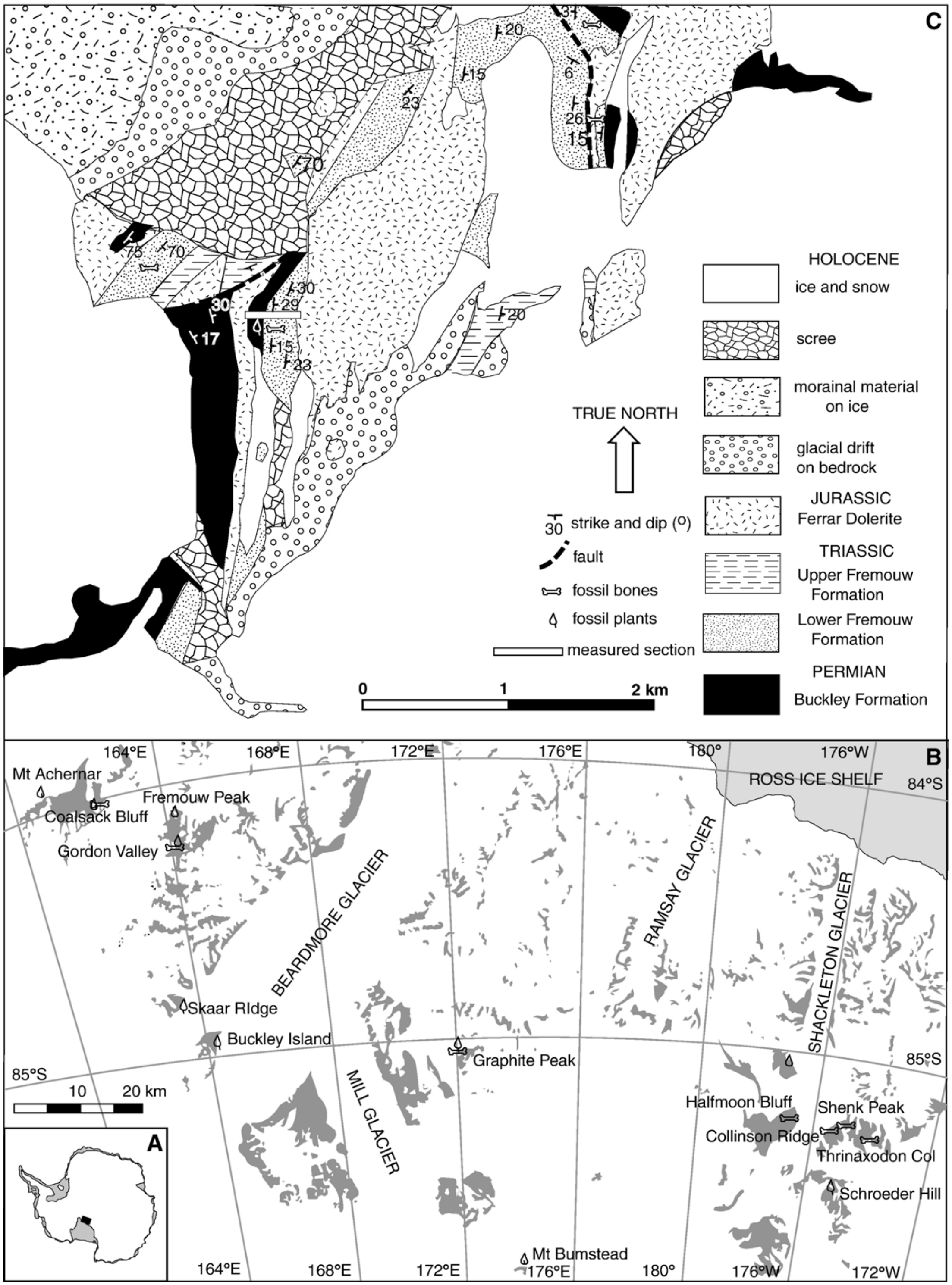

Fig. 1. Geological map (above) and location maps (below) for Coalsack Bluff, central Transantarctic Mountains, Antarctica. Maps modified from Collinson and Elliot (1984a,b).

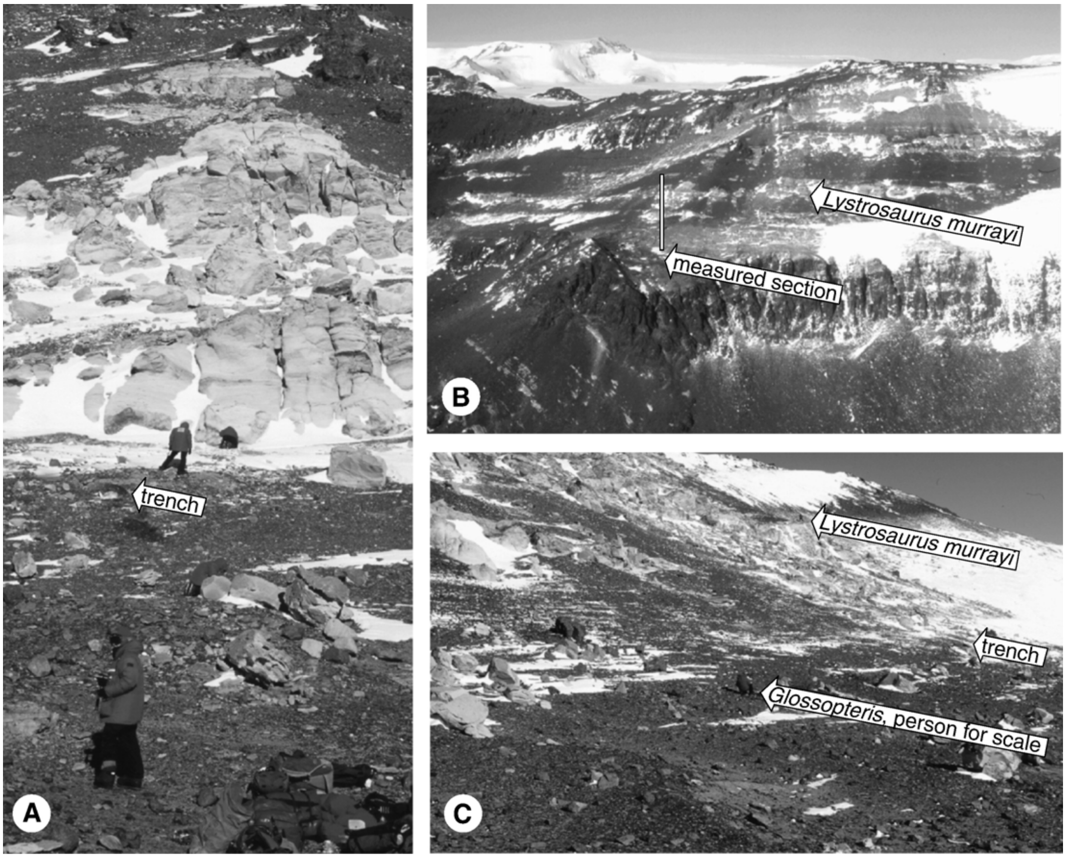

Fig. 2. Field photographs of Coalsack Bluff, central Transantarctic Mountains, Antarctica: A, view from base of measured section (Fig. 3), showing Late Permian shales in foreground overlain by cliff-forming Triassic sandstone; B, oblique airphoto of light-colored sediments of the measured section between thick dark dolerite dikes; C, view south along outcrop to Permian–Triassic boundary trenches and discovery site of *Lystrosaurus murrayi* (Colbert, 1974).

mature (bituminous to sub-bituminous, with local anthracites near dolerite intrusions (Coates et al., 1990), but regional burial alteration was not in excess of zeolite grade (Vavra et al., 1981; Vavra, 1989).

3. Field observations at Coalsack Bluff, Antarctica

Coalsack Bluff is a low nunatak about 8 km long by 5 km wide, largely of Early Jurassic Ferrar Dolerite (Collinson and Elliot, 1984a). This would be an unpromising site for fossils were it not for numerous small outcrops of coal measures of the Late Permian Buckley Formation and sandstones of the Triassic Fremouw Formation (Fig. 2). The contact between the two formations is best examined on the northwestern slope of the southwestern ridge of Coalsack Bluff (S84.23989° E162.29979°), where they are conformable and dip to the east (29° to strike 207° magnetic in 2003). Even here the contact between the Buckley and Fremouw Formations is covered by scree and ice, and had to be excavated in order to be examined (Figs. 2A, 4A).

The uppermost Buckley Formation in southwest Coalsack Bluff is a sequence of gray shales and coals (Fig. 3). These contain fragments of Permian leaves of the form genus *Glossopteris*, as well as the distinctive chambered roots (*Vertebraria australis*) and pycnoxylic wood (*Araucarioxylon*) thought to have belonged to the same kinds of swampland tree (Retallack and Dilcher, 1988). These fossils confirm palynological studies indicating a Late Permian age for the Buckley Formation at Coalsack Bluff (Tasch, 1978; Farabee et al., 1991). Only two of the 10 known Antarctic Permian paleosol types (Retallack and Krull, 1999) are represented in this short exposed section. The Susanne pedotype is a weakly developed paleosol (Fluvent of Soil Survey Staff, 1999), and represents early successional vegetation of clayey streamsides and lake margins. The Evelyn pedotype is a thick coal (Fibrist

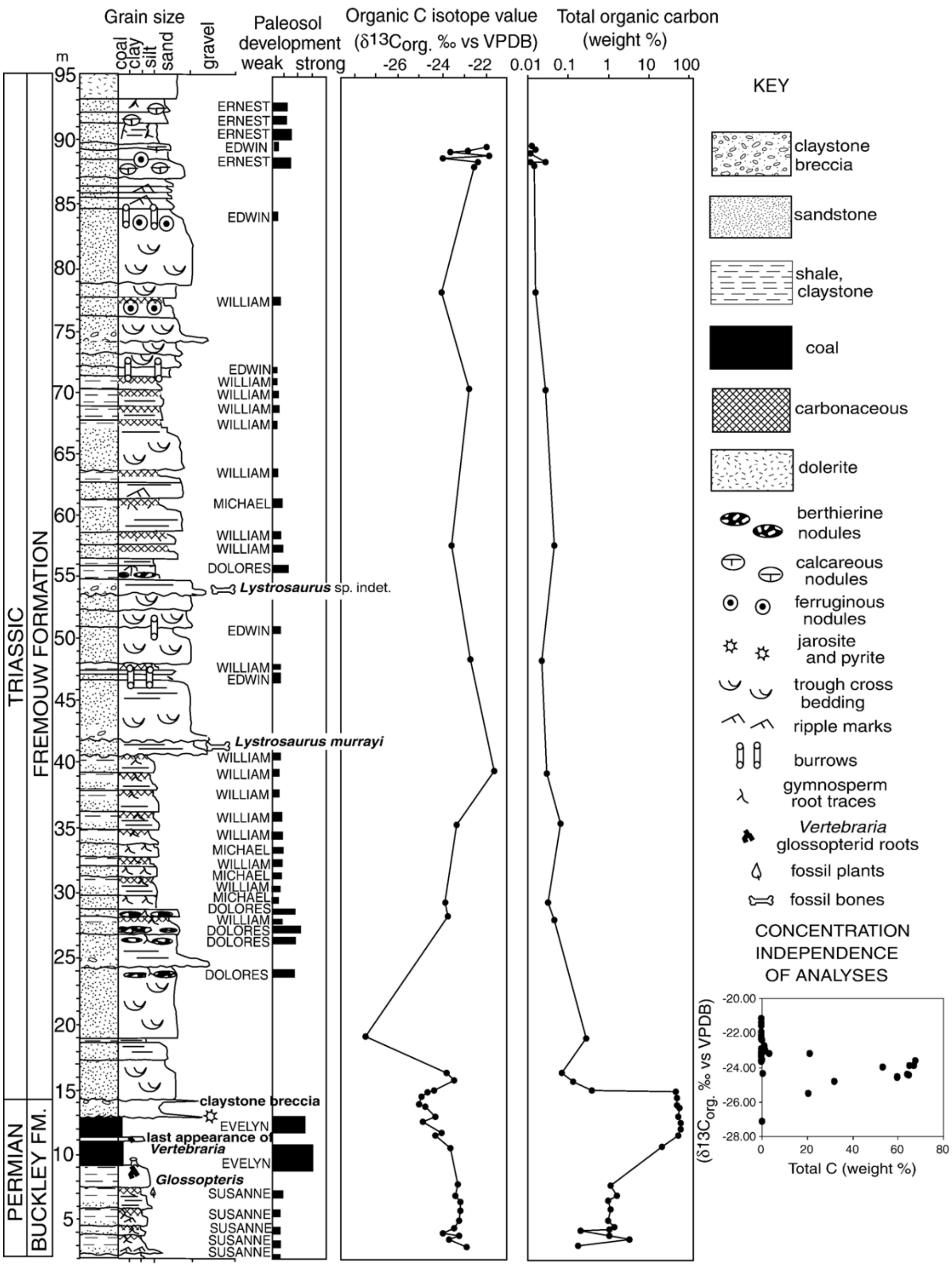

Fig. 3. Measured section of Permian–Triassic boundary at Coalsack Bluff, central Transantarctic Mountains. Paleosols in the sequence are named following Retallack and Krull (1999) with addition of Ernest pedotype named here, and represented by black boxes with thickness equal to that of the paleosol and width scaled to degree of soil development (following soil development scale of Retallack, 2001b). Organic carbon isotopic values and total organic carbon were determined using bulk rock samples.

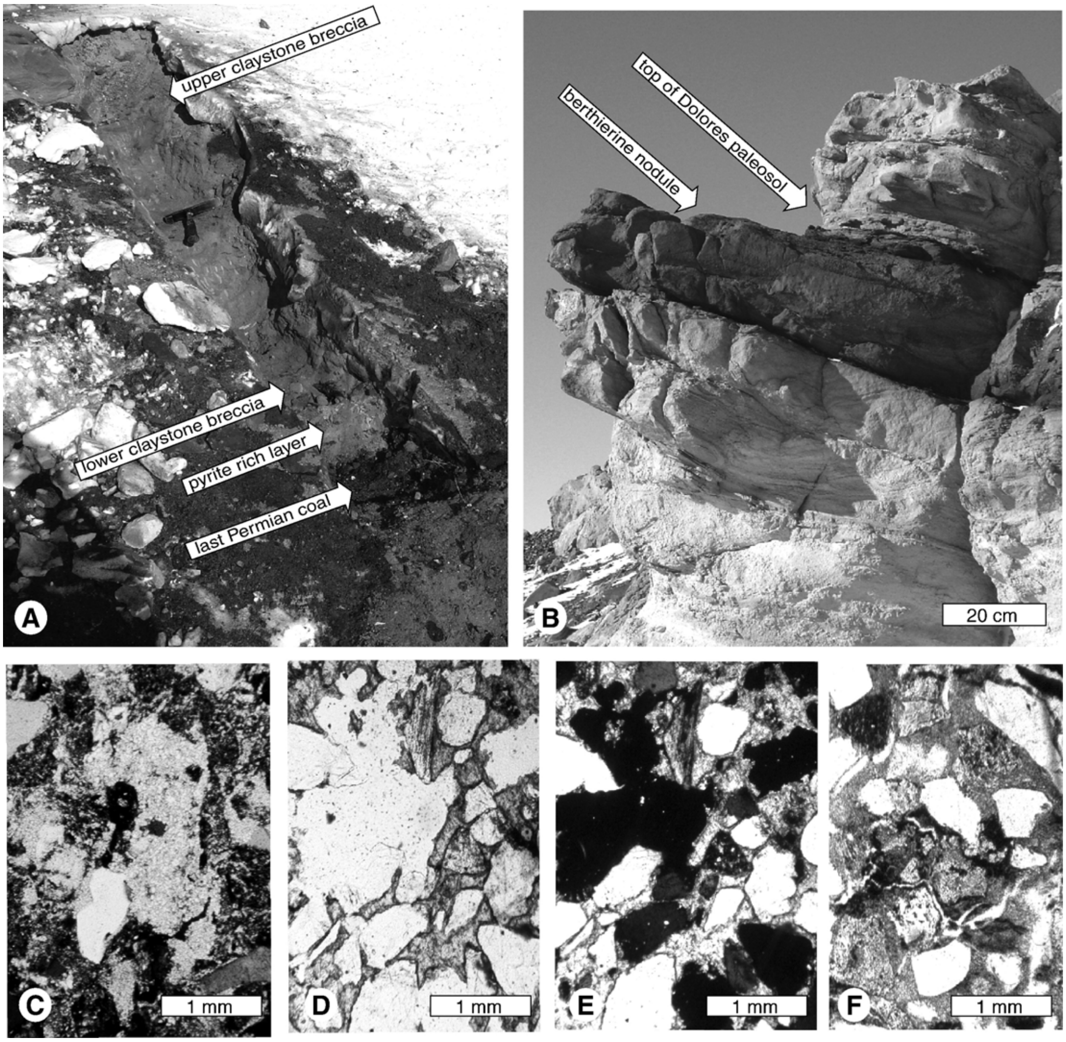

Fig. 4. Permian–Triassic boundary beds (A,C) and paleosols (B, D–F) in an excavated trench (A), outcrop (B) and petrographic thin sections (C–F) from Coalsack Bluff, Antarctica: A, claystone breccia above last Permian coal; B, Dolores paleosol at 24 m in measured section; C, mosepic claystone granule in boundary breccia under crossed nicols; D, groundwater calcrete of Ernest pedotype showing weathering rinds around grains in plane light; E, same view as D, but showing sparry calcite under crossed nicols; F, berthierine cement of nodule in Dolores paleosol. Hammer for scale in A, paleosol thickness in B is 40 cm, 1 mm scales for C–F. Sample numbers are R3122 for C, R3136 for E and D, and R3130 for F.

of Soil Survey Staff, 1999) and represents a long-lived, permanently waterlogged swamp.

The very top of the last coal (Evelyn pedotype) and the base of the overlying claystone breccia is yellow with jarosite, and dark with pyrite (Fig. 4A). Other Permian–Triassic boundary sections in Victoria Land (Retallack and Krull, 1999) and the Karoo Basin of Antarctica (Retallack et al., 2003; Maruoka et al., 2003) also are enriched in pyrite, and its weathering product jarosite, but the 14 cm pyritic zone at Coalsack Bluff is exceptionally massive.

Immediately above the last coal is a distinctive gray sandstone and claystone breccia, 70 cm thick, which differs from overlying trough-cross-bedded, quartz-rich sandstones of kinds common in Triassic rocks. This sandstone is not well exposed (Fig. 4A) but shows little bedding beyond parting lamination. The lowermost 17 cm of this bed is normally graded from claystone breccia to sandstone and the uppermost 12 cm of this bed is reverse graded from sandstone into claystone breccia. Petrography and sedimentology of this bed are unusual compared with overlying quartz-rich sandstones, and will be discussed further below.

The Fremouw Formation in southwest Coalsack Bluff is mainly light gray, quartz-rich sandstone. Bones can still be found disarticulated and worn within basal lags to these fluvial paleochannels. Although most of this material was referred to the genus *Lystrosaurus*, much of this material was not identifiable as particular species. Only two maxillae, one with a partial tusk, were identifiable to a particular species, *L. murrayi* (Colbert). We relocated the quarry, which is marked by a small stone cairn containing a soup tin with a written note. This is at 41 m above the last coal in this section (Fig. 3), not 82 m as shown in the section of Colbert (1974). The particular species and stratigraphic level is important because recent studies of the Karoo Basin of South Africa (Botha and Smith, 2004) reveal that some species of *Lystrosaurus* were Late Permian only (*L. maccaigi*), others survived from the latest Permian into the earliest Triassic (*L. curvatus*, *L. murrayi*) and others were Triassic newcomers (*L. declivis*). *L. murrayi* and *L. declivis* are the most common species well into the early Triassic but *L. curvatus* becomes extinct during the earliest Triassic (disappearing less than 20 m above, and probably less than 80 ka after the boundary, at the top of the Palingkloof member of the Balfour Formation of South Africa: Retallack et al., 2003). Thus *L. murrayi* 41 m above the last coal at Coalsack Bluff indicates latest Permian to early Triassic age.

All root traces in paleosols above the last coal at Coalsack Bluff are non-carbonaceous, as is usual for Antarctic Early Triassic paleosols, such as Dolores, William, Michael and Edwin pedotypes (Retallack and Krull, 1999). Dolores paleosols are striking in outcrop because they include large ellipsoidal nodules of hard, dark green, berthierine, often with a rusty red weathering rind. Berthierine is an unusual mineral in paleosols and indicates groundwater within the profile that was very chemically reducing (Sheldon and Retallack, 2002). Dolores paleosols are thin, sandy and have bedding planes and scattered root traces as in soils of streamsides supporting colonizing vegetation early in ecological succession after disturbance (Endoaquent of Soil Survey Staff, 1999). Such evidence of a short time of formation and colonizing vegetation also is found in William paleosols, which are clayey with green and carbonaceous surface horizons (Fluvent), in Michael paleosols, which are silty to sandy and light gray (Psamment), and in Edwin paleosols, which are sandy and quartz-rich, sometimes with small ferruginous nodules (also Psamment). Also weakly developed are sandy paleosols near the top of the measured section which include calcite nodules. No other calcareous paleosols have yet been found in Antarctica (Retallack and Krull, 1999), and these new kinds of profile are described below as the Ernest pedotype.

With its exceptionally thick (175 and 134 cm) coals with *Glossopteris*, boundary claystone breccia, and sandstones bearing *Lystrosaurus*, the Permian–Triassic boundary section at Coalsack Bluff, appears to have been at least as temporally complete a section as the one at Graphite Peak, central Transantarctic Mountains. There is little evidence of missing early Triassic section considering our correlation of Dolores paleosols and carbon isotope excursions throughout Antarctic sections (Retallack et al., 2005) with earliest Griesbachian (251 Ma), middle Griesbachian (250.5 Ma), mid-Smithian (247.6 Ma) and late Spathian (245 Ma) carbon isotopic anomalies in China (Payne et al., 2004). Nor can there be much Late Permian missing in the central Transantarctic Mountains because the very latest Permian *Playfordiaspora crenulata* palynomorph zone (of Foster, 1982) has been found in the last coal at Graphite Peak (Collinson et al., 2006), along with latest Permian to earliest Triassic *Protohaploxypinus microcorpus*, which has been reported also from Mt Achernar and other sites in the central Transantarctic Mountains (Farabee et al., 1991). While some sections of the Permian–Triassic boundary are disconformable, such as that at Portal Mountain, southern Victoria Land (Retallack et al., 2005), this disconformity does not include the entire Late Permian, as was once believed (Isbell and Cuneo, 1996; Isbell et al., 1999). The Permian–Triassic boundary in Antarctica is comparable with that in the Sydney Basin, Australia, where different parts of the basin have disconformities ranging in duration from 0.6 to 0.02 Ma, based on paleosol development, carbon isotope stratigraphy, palynology, event markers such as the fungal spike, sequence stratigraphy, and radiometric dating (Retallack, 1999a). Our studies reveal that Coalsack Bluff is a relatively complete and informative section for understanding end-Permian mass extinction.

4. Carbon isotope chemostratigraphy of Coalsack Bluff

Field observations of paleosols at Coalsack Bluff indicate that the Permian–Triassic boundary is somewhere between the last coal of the Evelyn pedotype with its carbonaceous roots, wood and leaves of glossopterids, and the lowest Dolores pedotype, with its rusty berthierine nodules and clayey root traces. There is little variation in the isotopic composition of latest Permian coals and shales at Coalsack Bluff, which in our 17 analyses averaged −23.08 ± 0.25‰ (one standard deviation). Carbon isotopic values reach a minimum (−24.62‰) within the claystone breccia overlying the last coal, then rebound (−23.12‰) toward normal Permian values in the overlying quartz sandstone (Fig. 3). A distinctive, thin, gray shale, 5.6 m above the last coal has the lowest carbon isotopic values of −27.19‰. While placement of the Permian–Triassic boundary at either the thin shale or claystone breccia could be defended, the abrupt drop in total organic carbon commonly associated with the boundary (Morante, 1996; Krull and Retallack, 2000) is immediately above the higher of the claystone breccias.

Decline in both total organic carbon and its carbon isotope value also pinpoints the Permian–Triassic boundary in claystone breccia above the last coal at Graphite Peak, Shapeless Mountain, Mount Crean and Allan Hills, Antarctica (Retallack et al., 2005). Our measurements of total organic carbon (Fig. 3) also support the field observation that Early Triassic root traces are clayey, in contrast to carbonaceous Late Permian root traces (Retallack and Krull, 1999). Coalsack Bluff thus validates an emerging pattern in carbon isotopic chemostratigraphy within Permian–Triassic boundary sections of Antarctica.

5. Petrography of Permian–Triassic boundary beds at Coalsack Bluff

The distinctive boundary sandstone with basal and capping claystone breccia at Coalsack Bluff has an unusual petrographic composition (Fig. 5; Table 1). Claystone clasts within the top and base of the gray sandstone include the following granule to small-pebble-sized, eroded soil fragments. Especially notable are silty claystone fragments with birefringence fabrics (mosepic and insepic plasmic fabrics of Brewer, 1976). Also found are volcanic rock fragments with ferruginized weathering rinds (diffusion sesquans of Brewer, 1976), indicative of marginal oxidation typical in soils, but possible also in well aerated sediments. This sandstone and breccia bed is thicker and more complex, but in many ways comparable with claystone breccias at the Permian–Triassic boundary throughout Antarctica, Australia and South Africa (Retallack et al., 1998, 2003). These sepic pedoliths have been interpreted as evidence for a pronounced interval of soil erosion at the Permian–Triassic boundary, because mosepic clasts are easily slaked in water (Retallack, 2005a). This whole unit with clayey granules is quite distinct (Table 1) from normal sandstones of the lower Fremouw Formation which average 67% quartz, 13% feldspar and 6% lithic grains (Barrett et al., 1986, and their table 13).

The distinctive gray clayey sandstone with its uppermost and lowermost claystone breccias and crude parting lineation appears to be an event deposit such as a debris flow. A fluvial origin is ruled out by the presence of soil clasts with sepic plasmic fabric, which cannot withstand immersion in water for more than a few minutes, let alone fluvial transport (Retallack, 2005a). Debris flows commonly have coarse-grained treads, tops and lateral levees in Oregon today, and some are as thick as 70 cm with sandy clayey central portions (Swanston and Swanson, 1976). Dry ravel deposits formed by soil peds rolling downhill dry after deforestation by forest fire (Gabet, 2003) can be this well sorted and fine-grained. Dry ravel deposits form talus cones and would have markedly different thickness along strike, as well as evidence of charcoal, not seen in either of two excavations across this bed at Coalsack Bluff (Fig. 2).

Impact and volcanic tracers have been recorded from Permian–Triassic claystone breccias at Graphite Peak including ^{3}He-bearing C^{60} fullerenes (Becker et al., 2001; Poreda and Becker, 2003) and carbonaceous-chondritic meteorite fragments (Basu et al., 2003). Modest iridium anomalies of as much as 59–80 ppt over a background of 20 ppt, an order of magnitude less than at the Cretaceous Tertiary boundary, have been found at the base of the last coal at Graphite Peak and in the claystone breccia at Mt Crean, Victoria Land (Retallack et al., 1998). Shocked quartz also has been reported from Graphite Peak and Mt Crean (Retallack et al., 1998). Reexamination by TEM of those grains from Graphite Peak studied with the spindle stage showed that they were unshocked, but had unusually closely spaced and subparallel subdomain boundaries (Langenhorst et al., 2005). The putative shocked grains are most likely stretched metamorphic grains from gneisses of the Nimrod Group (Gunner, 1983), rather than products of bolide impact. No clearly shocked quartz is now known from Antarctica, but investigation of iridium content, helium and sulfur isotopic composition, meteoritic and fullerene content of the Coalsack Bluff claystone breccias is ongoing in the laboratories of L. Becker (University of California Santa Barbara) and R. Poreda (University of Rochester). Euhedral bipyramidal quartz in claystone breccias at Graphite Peak (Retallack et al., 1998) is evidence of volcanic activity in the Andean-style volcanic arc presumed to have been to the northwest (Collinson et al., 1994). Fresh volcanic rock fragments in all the Antarctic Permian–Triassic boundary claystone breccias (Retallack, 2005a), including the one at Coalsack Bluff (Table 1), also attest to contemporaneous volcanic activity. Evidence of impact and volcanism discovered so far in Antarctic rocks is volumetrically minor compared with volcanic and soil components. These are soil destabilization deposits that entrained rare impact and volcanic components (Retallack, 2005a), and are very distinct from beds of impact ejecta (Izett, 1990; Sigurdsson et al., 1991; McCarville

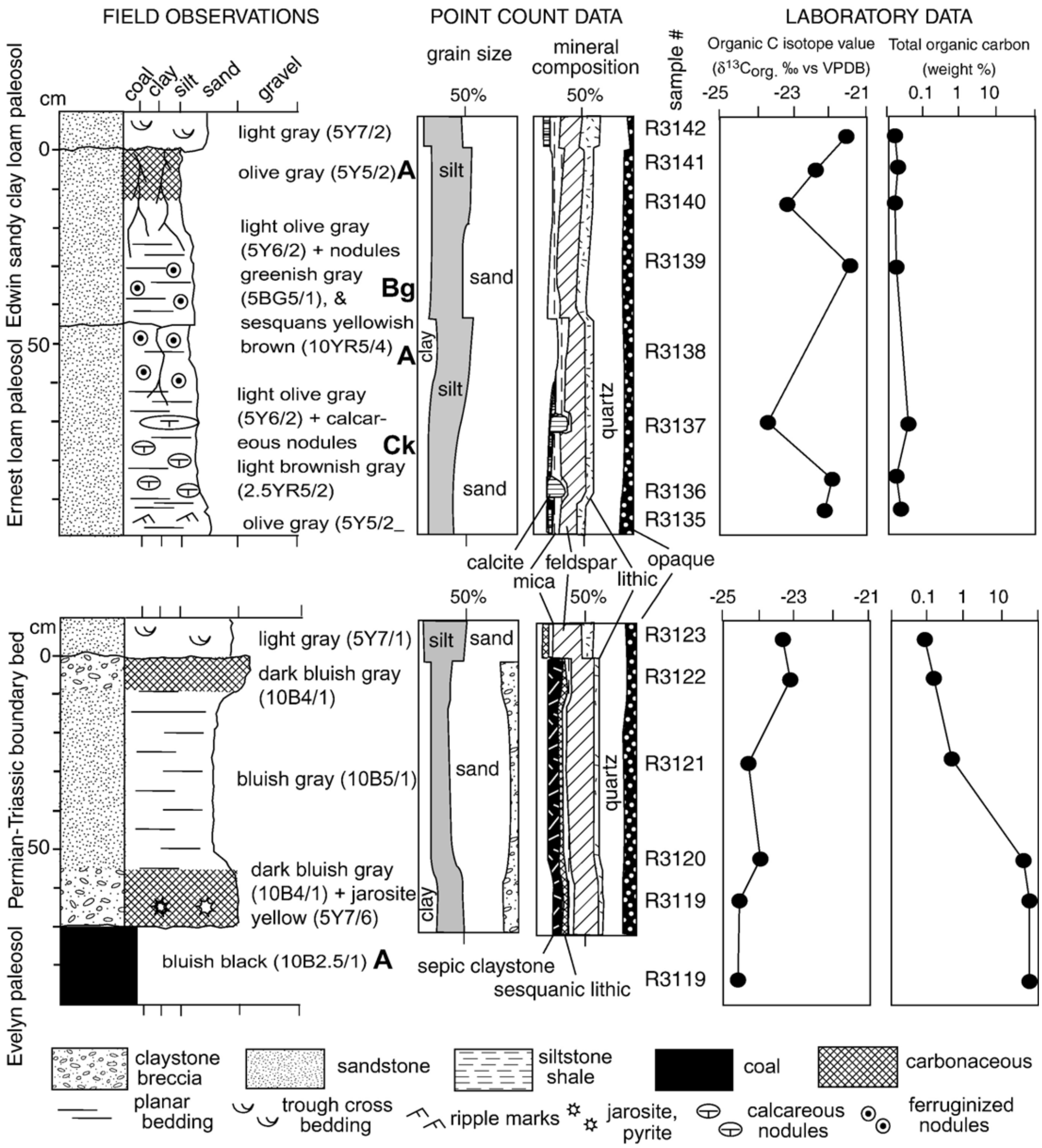

Fig. 5. Petrographic and geochemical data for Ernest and Edwin pedotypes at 88–90 m and for Permian–Triassic boundary bed at 13–15 m in measured section (Fig. 3) at Coalsack Bluff, Antarctica. Grain size and mineral composition determined by point counting of thin sections. Carbon isotopic value and total organic carbon content determined from bulk sample.

and Crossey, 1996) or volcanic tuff (Collinson et al., 1994; Elliot, 2000; Elliot and Hanson, 2001).

6. New paleosols at Coalsack Bluff and their carbon isotope profiles

The discovery of calcareous paleosols 83–89 m above the Permian–Triassic boundary at Coalsack Bluff was a surprise, because previously studied Antarctic Permian and Triassic paleosols were all non-calcareous, with the possible exception of rare sphaerosiderite (Retallack and Krull, 1999). Permian and Triassic calcareous paleosols are known from the Karoo Basin of South Africa, but these are thought to have formed in much less humid paleoclimate than the non-calcareous paleosols of Antarctica (Retallack et al., 2003).

Calcareous paleosols of Coalsack Bluff stand out in the field, and are here termed the Ernest pedotype, after Ernest Shackleton, legendary Antarctic explorer. Ernest paleosols consist of laminated sandstones, with sparse clay-replaced,

Table 1
Mineral composition (%) of sandstone bed above last coal at Coalsack Bluff

Specimen	R3119	R3120	R3121	R3122	R3123
Quartz	23.6	27.8	28.0	29.8	33.0
Opaque	7.2	6.6	5.4	7.0	6.2
Feldspar	28.0	25.4	27.6	19.4	26.0
Clay	18.0	16.6	12.8	13.6	11.2
Mica	2.8	7.8	5.0	3.0	3.6
Hornblende	1.0	1.4	2.0	0	2.4
Fresh volcanic rock fragments	3.8	3.6	3.6	6.4	13.6
Sesquanic (oxidized) volcanic rock fragments	6.6	4.6	3.6	9.0	4.0
Insepic clayey soil fragments	6.4	3.6	7.0	5.6	0
Mosepic clayey soil fragments	2.6	2.6	5.0	6.2	0

root traces, and shallow tabular beds or platy nodules of calcite (Fig. 5). The prominence of bedding is unusual for paleosols with well developed calcareous nodules, because pedogenic nodules of this size and thickness take many thousands of years to form (Retallack, 2005b), and roots and burrows over such a length of time destroy original bedding planes of parent sediment (Retallack, 2001b). Petrographic study confirms that these are not pedogenic nodules of Aridisols, which have replacive micrite and displacive spar (Retallack, 1997a). The Coalsack Bluff carbonates have a very different microscopic structure of sparry calcite filling the interstices of quartz and other grains (Fig. 4D–E). Especially striking is a thin ferruginized rind (diffusion sesquan of Brewer, 1976) around both individual grains and groups of grains (Fig. 4D), separating them clearly from the void-filling calcite. This indicates calcite precipitation following oxidation of pores. The calcite fill of large vugs indicates precipitation before appreciable burial compaction. These fabrics are similar to those of groundwater calcite and travertine, in which carbonate is precipitated from pore waters (Nash and Smith, 2003; Retallack et al., 2002).

Immaturity of the Ernest and associated Edwin pedotype is also revealed by large and erratic changes in carbon isotopic composition (Fig. 4). In contrast, well developed forest soils have a smooth curve of carbon isotope values, negative near the top because of fresh inputs of litter, a few permil more positive in the Bt horizon due to bacterial decay of organic matter, and negative near the base from water-soluble fresh leachates. This pattern was demonstrated in Antarctic Triassic paleosols presumed to have been forested, and served to differentiate them from other kinds of paleosols (Krull and Retallack, 2000). The transition from early successional paleosols with erratic carbon isotopic profiles to smoother carbon isotope profiles in more strongly developed paleosols is clear from Antarctic Early Triassic paleosols.

Considering their very weak development, Ernest paleosols are best classified as Entisols in the US taxonomy (Soil Survey Staff, 1999). Their ferruginization of grain boundaries and calcite precipitation from groundwater within 50 cm of the ground surface mark them as Psammaquents (of Soil Survey Staff, 1999). In the Food and Agriculture Organization (1974) classification Ernest paleosols are more like Calcaric Gleysols. These are soils of waterlogged and disturbed sedimentary environments, probably swales within a sandy braid plain. They represent a relatively short period of soil formation, probably not in excess of a century. Observed root traces include relatively thin tap roots and laterals like those common in equisetaleans, such as *Townroviamites brookvalensis* known as fossils at comparable stratigraphic levels on Mt Rosenwald (Retallack et al., 2005). Such vegetation would have been an herbaceous thicket of standing water and shallow groundwater.

Entisols and Gleysols are not diagnostic of a particular regional climate or vegetation, and are very restricted in temporal and geographic distribution. Other paleosols of the lower Fremouw Formation have been compared (by Retallack and Krull, 1999) with soilscapes of the lower Amur River basin of far-eastern Russia (map unit Lg1-2b of Food and Agriculture Organization, 1978a), rolling plains near Palmerston, North Island, New Zealand (Lg22-2a of Food and Agriculture Organization, 1978b), and the Traun River between Braunau and Wells, Austria (Lg44-2/3a of Food and Agriculture Organization, 1981). Of these choices, only the Austrian soilscape has inclusions of Gleysols comparable with Ernest paleosols. Calcareous Pleistocene gravels forming the fortified crags in Salzburg, widely used in local baroque architecture (Stummer, 1936; Tichy et al., 1985), are a modern analog on a much greater scale of topographic relief and thickness than the groundwater calcretes of the Ernest pedotype. Such groundwater calcrete is compatible with indications from other early Triassic paleosols of humid temperate paleoclimate (Retallack and Krull, 1999). Comparable modern Austrian soilscapes are forested with deciduous broadleaf oak (*Quercus petraea*) and hornbeam (*Carpinus cordata*). Climate near Salzburg is cool temperate (mean annual temperature 8.1 °C, with mean for January −2.5 °C and for June 17.8 °C), and humid (mean annual precipitation 1278 mm: Müller, 1982). Such a warm and humid climate is remarkable for this part of Antarctica, which was in the interior of a supercontinent at very high paleolatitude

(Scotese, 1994), and supports the idea of a post-apocalyptic early Triassic greenhouse (Retallack, 1999a).

7. Antarctic Permian–Triassic sequence of events

Antarctica shows the following detailed sequence of Permian–Triassic events. The last Permian coal persisted after a slight (80 ppt) iridium anomaly detected at the base of the last thick coal at Graphite Peak (Retallack et al., 1998), comparable with iridium anomalies elsewhere near the Permian–Triassic boundary (Oddone and Vannucci, 1988; Holser et al., 1989). At Graphite Peak, Coalsack Bluff and Portal Mountain, carbon isotopic composition begins to decline 10,000 years before end of the last coal and the total extinction of the *Glossopteris*-dominated ecosystem at the globally synchronous isotopic nadir (Retallack et al., 2005; Bowring et al., 1998). In the Allan Hills, Mt Crean and especially Coalsack Bluff, the top of the last coal is marked by increased abundance of pyrite, variably oxidized to jarosite and hematite. Directly overlying the last coal at most localities is a distinctive claystone breccia, with clasts of sepic plasmic fabric identical to that found in Permian paleosols (Retallack et al., 1998; Retallack, 2005a). These claystone breccias contain rare indicators of active volcanism, such as fresh volcanic rock fragments and bipyramidal quartz (Retallack et al., 1998), and indicators of bolide impact, such as ^{3}He-bearing C^{60} fullerenes (Becker et al., 2001; Poreda and Becker, 2003) and carbonaceous-chondritic meteorite fragments (Basu et al., 2003). None of the characteristic Permian paleosols is found above this level, where the most common paleosols of the Dolores pedotype have abundant nodules of berthierine, non-carbonaceous root traces and very low total organic carbon contents. A diversity of other pedotypes include weakly developed paleosols of sandy, clayey and waterlogged stramsides, as well as paleosols of wooded and forested lowlands (Retallack and Krull, 1999).

These various observations can be interpreted as consequences of initial extraterrestrial impact (modest iridium anomalies of Retallack et al., 1998), which was not sufficiently catastrophic to curtail peat formation or extinguish *Glossopteris*. Carbon isotope values in coals subsequently declined erratically to such low values that they can only be explained by successive massive release of methane clathrates from marine continental shelves or permafrost (Krull et al., 2000, 2004). Pyrite enrichment at the Permian–Triassic boundary, especially obvious at Coalsack Bluff, is highly unusual for non-marine strata, and may reflect atmospheric pollution with sulfur oxide gases from bolide impact or volcanism (Maruoka et al., 2003). At the nadir of carbon isotopic decline, peat-forming *Glossopteris* swamps became extinct (coal gap of Retallack et al., 1996), and lowland forest dieback ushered in a dramatic episode of soil erosion (claystone breccias of Retallack, 2005a). Fullerenes (Poreda and Becker, 2003) and meteoritic fragments (Basu et al., 2003) of these debris flows of destabilized soil are little weathered, and may indicate fresh extraterrestrial impact, perhaps from “Bedout Crater” of Western Australia (Becker et al., 2004: though evidence for that crater is disputed by Renne et al., 2004; Wignall et al., 2004). Explosive volcanic activity in the Gondwanide margin andesitic arc also continued, as represented by bipyramidal volcanic quartz in boundary breccias (Retallack et al., 1998). Earliest Triassic paleosols are more deeply weathered than Late Permian ones, indicating a warmer and wetter climate (Retallack and Krull, 1999), and their berthierine nodules indicate unusually low soil oxygen content (Sheldon and Retallack, 2002; Huggett et al., 2003). Within this post-apocalyptic greenhouse, Antarctica was colonized by conifers such as *Voltziopsis* and seed ferns such as *Lepidopteris* immigrating from Australia or Madagascar to the north (McLoughlin et al., 1997; Retallack, 2002a). *Lystrosaurus* also may have migrated south from South African deserts (Retallack et al., 2003) once swamp woodlands of Antarctica and Australia were replaced with lowland conifer forests (Retallack, 1996; Retallack and Hammer, 1998). Finally, all the Antarctic sites were overrun with massive paleochannel sandstones of braided streams, resulting from widespread lowland deforestation (Ward et al., 2005; Michaelson, 2002).

8. Methane outburst scenario for end-Permian mass extinction

A newly recognized potential player in the carbon cycle are methane hydrates, which are solids composed of CH_4 and H_2O that result from the anaerobic metabolism of organic carbon by chemoheterotrophic archaea in marine sediments. The total present-day mass of carbon stored as methane hydrate in continental shelf sediments and permafrost may be as large as 11,000 Gt of C (Kvenvolden, 2000), 3000 Gt (Buffett and Archer, 2004), or as small as 500 to 2500 Gt (Milkov, 2004). Much of the methane is trapped in ice of subsea pore spaces after migrating upwards through sediments, and these ices can be mapped as a seismic bottom-simulating reflector (Yuan et al., 1996). Massive methane outbursts require an efficient release mechanism, because it is very effectively trapped within sediments and permafrost, and annual sinks of methane are currently of the order of 5 Gt (Khalil, 2000). Catastrophic releases by volcanism, bolide impact or continental shelf collapse would degas large amounts of methane directly to the atmosphere (Jahren, 2002; Retallack and Krull, 2006). There is also the possibility of a runaway release triggered by minor sea level fall, or rising temperature (Kvenvolden, 2000). Runaway release can be envisaged because methane is 30 times more potent as a greenhouse gas than carbon dioxide, to which most methane oxidizes in the atmosphere with 7–24 years (Khalil, 2000). Minor warming could thus by positive feedback cause further methane release and runaway warming. Methane dissociation from the oceanic hydrate reservoir would first saturate local seawater, and then excess methane would migrate up the water column and be released into the atmosphere. Marine saturation with methane and carbon dioxide may prevent catastrophic runaway from minor releases (Dickens, 2001) Fig. 6.

The key to recognizing methane outbursts of the past (Dickens et al., 1995) and plumes of the present (Nisbet, 2002) is its unusual carbon isotope composition. Carbon isotopic ($\delta^{13}C$) values of −60 to −110‰ are only known from biologically-produced methane (Khalil, 2000), and values of −37 to −55‰ from either biological or coalbed thermogenic methane (Scott et al., 1978). Methane outburst from ocean hydrates is best documented during the latest Paleocene (55.6 Ma) from a negative excursion (−2.5‰) in the marine carbonate record (Dickens et al., 1995, 1997). Atmospheric rather than merely oceanic pollution with methane is demonstrated by synchronous negative carbon isotope excursions of similar magnitude in soil carbonate in Wyoming (Koch et al., 1992, 1995) and terrestrial organic matter in France (Stott et al., 1996). The global biogeochemical response to such an event may be extremely rapid, with atmospheric isotopic change within 10,000 years and recovery for 100,000 years or more (Norris and Rohl, 1999). The Paleocene/Eocene boundary was a time of global climate change, with a rapid 4 to 8 °C increase in deep-ocean, high latitude and continental temperatures inferred from changes in oxygen isotopic composition of marine carbonates (Kennett and Stott, 1991; Zachos et al., 1993). Comparable temperature change on land is confirmed by oxygen isotopic anomalies in teeth of land animals (Fricke et al., 1998) and by leaf margin analysis of fossil floras in Wyoming (Wing, 1998). Increased precipitation and seasonality of precipitation is revealed by increased depth and spread of carbonate nodules within paleosols of Utah (Retallack, 2005b), and increased terrestrial chemical weathering can be inferred from osmium isotope records in the ocean (Ravizza et al., 2001). There were major turnovers in terrestrial and marine flora and fauna at this time (Hooker, 1996; Thomas and Shackleton, 1996). Volcanic intrusion (Svensen et al., 2004) and comet impact (Kent et al., 2003, 2004) have been proposed as triggers for catastrophic terminal Paleocene methane outbursts, but submarine landslides and faulting may also have played a role (Reguera, 1998; Katz et al., 2001). Large methane dissociation events have also been identified in the early Jurassic *Harpoceras falciferum* ammonite zone of the

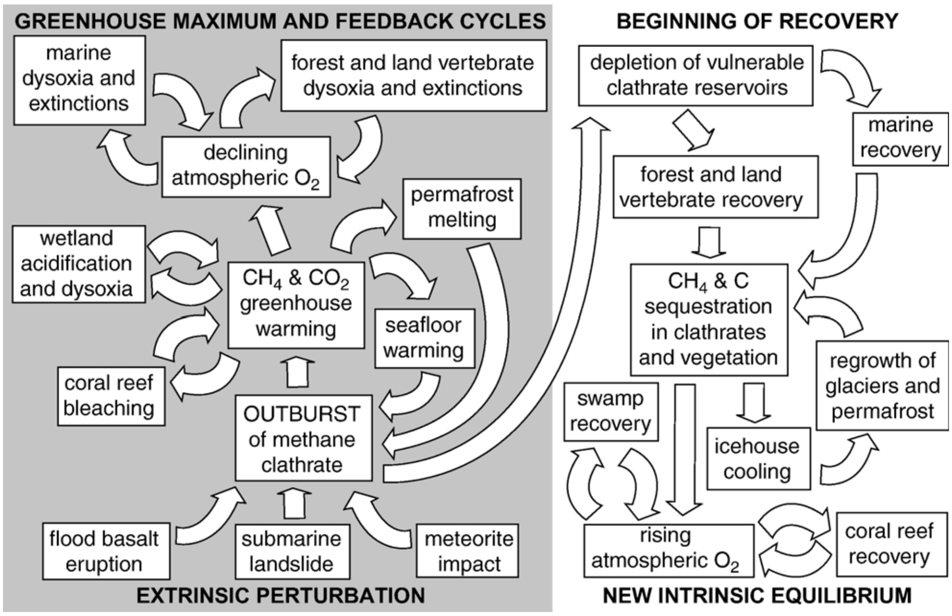

Fig. 6. Consequences and feedbacks for massive outburst of methane from permafrost and subsea clathrates (left), and for recovery from such carbon cycle crises (right), as envisaged for the Permian–Triassic mass extinction.

Toarcian (Hesselbo et al., 2000; McElwain, 2005), and early Cretaceous Selli Event of the *Leopoldina cabri* foraminiferal zone of the Aptian (Jahren et al., 2001; Jenkyns, 2003).

A methane outburst scenario for mass extinction at the Permian–Triassic boundary was first confirmed by discovery of unusually light carbon isotopic composition of earliest Triassic organic matter in Antarctic paleosols (Krull and Retallack, 2000) and New Zealand marine sequences (Krull et al., 2000). Such definitively methanogenic isotopic excursions have since been found elsewhere in earliest Triassic fluvial sediments (de Wit et al., 2002; Sarkar et al., 2003), pedogenic carbonate (Ward et al., 2005), and marine carbonates (Newton et al., 2004). Mass balance calculations show that oxidation of non-methanogenic biomass (−35‰ to −20‰), cannot account for isotopic excursions of the magnitude observed at the Permian–Triassic boundary (Krull et al., 2000; de Wit et al., 2002; Berner, 2002). The excursions are also too large to be explained by inputs of carbon from mantle degassing (−7 to −5‰; Dickens et al., 1995). Meteorites (−47 to +1100‰; Grady et al., 1986; Pillinger, 1987) or comets (down to−120‰; Jessberger, 1999; Messenger, 2000) rarely have suitable isotopic composition, but would also come with more iridium and helium than observed at the Permian–Triassic boundary (Becker et al., 2001; Farley and Mukhopadhyay, 2001). The largest isotopic excursions are in high latitudes and on land in Antarctica, Greenland, South Africa and India. Less severe isotopic excursions are found across the Permian–Triassic boundary in deep marine and tropical sections of Canada, Japan, China and Europe (Krull et al., 2004; Retallack and Krull, 2006). This has been taken as evidence for uneven geographic mixing of methane (Krull et al., 2004; Retallack and Krull, 2006). Even within Antarctica, the magnitude of the isotopic excursion varies from section to section, as if methane sources and atmospheric plumes were localized (Retallack and Krull, 2006).

As for the terminal Paleocene, it is difficult to choose between supporting evidence for potential mechanisms of methane release at the Permian–Triassic boundary: volcanic eruption, dolerite intrusion, submarine landslide and marine faulting. Siberian Trap lavas beginning at the Permian–Triassic boundary (Renne et al., 1995; Mundil et al., 2001; Reichow et al., 2002) could have liberated substantial amounts of methane by direct degassing of greenhouse-inducing CO_2 and H_2O, by thermogenic release and generation of coalbed methane in intruded coal measures, and by melting of permafrost by large flows. Estimated volumes of Siberian Trap gases fail to explain the full range of end-Permian atmospheric devastation (Kerrick, 2001; Wignall, 2001), but such gases cannot be ruled out as a contributory cause of the crisis (Benton, 2003). Siberian Traps erupted into coal basins (Czamanske et al., 2002), and their feeder and associated intrusions could have liberated and thermogenically generated coalbed methane of isotopically light composition in large volumes, as postulated for the Toarcian methane release event (McElwain, 2005). There is paleosol evidence of permafrost in *Glossopteris*-dominated Permian peatlands of the Triassic south polar region (Krull, 1998, 1999; Retallack, 1999b), and although such studies have not yet been attempted on paleosols associated with the Siberian Traps, they were erupted at high northern latitudes (Scotese, 1994). A huge (500 km diameter) crater (Bedout, Western Australia, has now been dated at 250.1±4.5 Ma (Gorter, 1996; Becker et al., 2004), but remains controversial (Wignall et al., 2004; Renne et al., 2004). Also disputed is evidence of Permian–Triassic shocked quartz (Langenhorst et al., 2005), iridium anomalies in the range 59–80 ppt, and fullerenes with extraterrestial noble gases (Farley and Mukhopadhyay, 2001; Koeberl et al., 2004). Less easy to dismiss are meteorite fragments at the Permian–Triassic boundary at Graphite Peak (Basu et al., 2003), where their preservation can be attributed to early diagenetic berthierine nodules (Sheldon and Retallack, 2002). A final methane release mechanism is from large submarine slides, as represented by the Permian–Triassic Little Ben Sandstone of New Zealand (Krull et al., 2000) and the carbonate olistostrome of Kaki Vigla, on the island of Salamis, Greece (Baud et al., 1989), which both contain profound carbon isotopic excursions. Triggering of methane release by transform faulting, subduction zone earthquakes, or regional uplift under superplumes is also plausible, as argued for Aptian methane outburst (Jahren et al., 2001; Jahren, 2002).

Carbon isotope excursion magnitudes matter, because they allow quantitative estimates of outburst volumes and effects. The average isotopic excursion for organic carbon from 30 analyzed Permian–Triassic sections worldwide (Retallack and Krull, 2006) is −6.4±4.4‰ (one standard deviation), which requires release to the atmosphere of at least 622±589 Gt ($=10^{15}$ g) of CH_4 (≈467 Gt of C from methane: calculated using algorithms of Jahren et al., 2001, from starting value of Retallack, 2001a, 2002b, recalculated following Wynn, 2003). Earliest Triassic methane release and oxidation thus created an atmosphere of at least 1684±916 ppmV CO_2, a value comparable with estimates from stomatal index of earliest Triassic seed ferns (Retallack, 2002a). This amount of methane is no more than 6–100% of estimated inventories of methane hydrates in the world (Kvenvolden, 2000; Milkov, 2004). These simplistic mass balance calculations support numerical models of the Permian–Triassic methane outburst event by de Wit et al. (2002) and Berner (2002), but not extreme methane outbursts postulated by Ryskin (2003). Likely kill mechanisms in a methane outburst catastrophe explain observed selectivity of the Permian–Triassic mass extinctions. In the ocean, excess CO_2 (hypercapnia), which would form by oxidation of CH_4, has been suggested to explain preferential end-Permian extinction of marine invertebrates with heavily calcified skeletons, poor respiratory and circulatory systems and low basal metabolic rate (Knoll et al., 1996). Carbon dioxide saturation also has been invoked to explain early Triassic calcite seafloor cements (Heydari and Hassanzadeh, 2003). Some degree of hypoxia (O_2 deficit) also may explain early Triassic unbioturbated, pyritic and carbonaceous marine shales and cherts (Kajiwara et al., 1994; Kakuwa, 1996; Isozaki, 1997; Twitchett et al., 2001; Wignall et al., 2005), and biomarkers such as isorenieratane in earliest Triassic shallow marine rocks (Grice et al., 2005).

On land, end-Permian anoxia in soils already marginally aerated within poorly drained lowland and coastal regions would kill roots by suppressing root respiration (Sheldon and Retallack, 2002). Such lowland soil anoxia and post-apocalyptic greenhouse tallies with several unusual features of earliest Triassic paleosols: their extreme fluctuations in carbon isotopic depth functions (Krull and Retallack, 2000), their unusually strong chemical weathering compared with physical weathering, high paleolatitudinal distribution of deeply weathered soils such as Ultisols (Retallack and Krull, 1999), and shallow nodules of such oxygen-intolerant minerals as berthierine and siderite within formerly porous sandy paleosols (Retallack, 1999a, 1997b; Sheldon and Retallack, 2002). Aquatically adapted glossopterid roots of *Vertebraria* were extinguished at the Permian–Triassic boundary throughout the Gondwana supercontinent (Retallack and Krull, 1999). Peat-forming ecosystems of austral glossopterids and boreal ruflorian cordaites were destroyed utterly at the end of the Permian, and coals contained very different plants when peat-forming communities re-evolved during the Middle Triassic (Retallack, 1995; Retallack et al., 1996). Terminal–Permian lowland woody plant dieback is indicated by unusually abundant fungal spores, preferential extinction of gymnosperms compared with pteridophytes, and shifting histological and chemical composition of palynodebris (Visscher et al., 1996), although some of the supposed fungal hyphae were more likely aquatic algae (Afonin et al., 2001; Foster et al., 2002). Destruction of woody plants in lowland sedimentary environments is also indicated by the abundance of weakly developed earliest Triassic paleosols (Retallack and Krull, 1999; Retallack, 1999a), extensive claystone breccias from upland soil erosion (Retallack, 2005a), and by the spread of earliest Triassic braided streams (Ward et al., 2000; Michaelson, 2002). The most successful early Triassic plants were isoetalean lycopsids, with shallow, hollow rootlets, adapted to poorly aerated soils (Retallack, 1997c).

For land vertebrates, the earliest Triassic atmosphere modeled by Berner (2002) had an oxygen content comparable to that found at 6000 m today, and many creatures would have died by pulmonary edema and acidosis, in a syndrome comparable with "mountain sickness" (Retallack et al., 2003). Large areas of the earth at high elevations would have been sterilized of vertebrates (Huey and Ward, 2005), and only those creatures pre-adapted to oxygen stress would have survived. Most reptiles and amphibians disappeared at the Permian–Triassic boundary (Smith and Ward, 2001; Ward et al., 2005), and among the few survivors was *Lystrosaurus*, a burrowing detritivore with a cosmopolitan distribution (Retallack, 1996; Retallack and Hammer, 1998; Lucas, 1998). With its short snout, bony secondary palate, barrel chest, and high neural spines, *Lystrosaurus* was better adapted than most other Permian reptiles to oxygen shortages within the burrows in which it is often found (Retallack et al., 2003). *Lystrosaurus*, like its much later mammalian ancestors, may also have had a greater capacity for acclimatization than other latest Permian vertebrates, which may have been as limited as modern frogs in ability to acclimatize (Engoren and Retallack, 2004).

We have emphasized the methane outburst hypothesis here because its exposition and ramifications are new (Krull and Retallack, 2000; Berner, 2002; Heydari and Hassanzadeh, 2003), but there is still an open season on ideas about the Permian–Triassic life crisis, with many competing hypotheses. For example, Kaiho et al. (2001) and Becker et al. (2004) propose that a giant impact caused the mass extinction as a preplay of the popular scenario of "*Tyrannosaurus rex* and the crater of doom", with a global dust cloud and chilling followed by post-apocalyptic greenhouse (Alvarez, 1997). Even if all the disputed evidence for terminal Permian impact were accepted, such an impact was still smaller than at the Cretaceous–Tertiary boundary, where extinctions were much less catastrophic (Retallack et al., 1998). Alternatively, Benton (2003), Benton et al. (2004) and Ward et al. (1995) argue for a gradual extinction due to atmospheric contamination with carbon dioxide and sulfur oxide gases from the giant flood basalt eruptions of the Siberian Traps. Unfortunately, even the most optimistic volumes of the Siberian traps and their likely content of SO_2, SO_3, and CO_2 do not create an atmospheric crisis of the magnitude observed (Kerrick, 2001; Wignall, 2001; Berner, 2002). Finally, Hallam and Wignall (1997), Kidder and Worsely (2004), Wignall et al.

(2005), Grice et al. (2005), and Kump et al. (2005) argue that the extinctions were produced by oceanic stagnation and anoxia spreading into the photic zone, perhaps with release to the atmosphere of sulfur gases. This hypothesis fails to explain the dramatic decline in total organic carbon in earliest Triassic marine rocks (Morante, 1996; Krull et al., 2004), which should be more carbonaceous by proposed productivity stagnation models.

None of these scenarios preclude a role for methane, because oxidation of sufficient amounts of methane might induce oceanic anoxia, and volcanism, tectonism and impact could release large volumes of methane. We do not imagine that these various scenarios will be reconciled any sooner than comparable debates concerning the Cretaceous–Tertiary mass extinction, but we do suggest that methane was a key element during the greatest of all mass extinctions at the Permian–Triassic transition.

Acknowledgements

We thank Bill Hagopian for laboratory assistance. Shaun Norman, Luann Becker, Scott Robinson, and Carolyn Phillips aided with fieldwork, as did Kevin Kililea in the 1996 Shackleton base-camp and Curt Labombard in the 2003 Beardmore base-camp. Funded by NSF grants OPP0230086 to GJR and OPP0229136 to AHJ.

References

Afonin, S.A., Baranova, S.S., Krassilov, V.A., 2001. A bloom of *Tymnpanicysta* Balme (green algae of zygnematalean affinities) at the Permian–Triassic boundary. Geodiversitas 23, 481–487.

Alvarez, W., 1997. *T. Rex* and the Crater of Doom. Princeton University Press, Princeton. 185 pp.

Barrett, P.J., Baillie, R.J., Colbert, E.H., 1968. Triassic amphibian from Antarctica. Science 161, 460–462.

Barrett, P.J., Elliot, D.H., Lindsay, J.F., 1986. The Beacon Supergroup (Devonian–Triassic) in the Beardmore Glacier Area, Antarctica. In: Turner, M.D., Splettstoesser, J.F. (Eds.), Geology of the Central Transantarctic Mountains, Antarctic Research Series. American Geophysical Union, vol. 36, pp. 339–428.

Basu, A.R., Petaev, M.I., Poreda, R.J., Jacobsen, S.B., Becker, L., 2003. Chondritic meteorite fragments associated with the Permian–Triassic boundary in Antarctica. Science 302, 1388–1392.

Baud, A., Magaritz, M., Holser, W.T., 1989. Permian–Triassic of the Tethys: carbon isotope studies. Geologische Rundschau 78, 649–677.

Becker, L., Poreda, R., Hunt, H.G., Bunch, T.E., Rampino, M., 2001. Impact event at the Permian–Triassic boundary: evidence from extraterrestrial noble gases in fullerenes. Science 291, 1530–1533.

Becker, L., Poreda, R., Basu, A.R., Pope, K.O., Harrison, T.M., Nicholson, C., Iasky, I.R., 2004. Bedout: a possible end-Permian impact crater offshore of northwestern Australia. Science 304, 1469–1476.

Benton, M.J., 2003. When Life Nearly Died. Thames and Hudson, New York. 336 pp.

Benton, M.J., Tverdokhlebov, V.P., Surkov, M.V., 2004. Ecosystem remodelling among vertebrates at the Permian–Triassic boundary in Russia. Nature 432, 97–100.

Berner, R.A., 2002. Examination of hypotheses for the Permo–Triassic boundary extinction by carbon cycle modeling. U.S. National Academy of Sciences Proceedings 99, 4172–4177.

Botha, J., Smith, R.M.H., 2004. *Lystrosaurus* species composition across the Permian/Triassic boundary in South Africa. Journal of Vertebrate Paleontology Supplement 3, 40A.

Bowring, S.A., Erwin, D.H., Jin, Y.G., Martin, M.W., Davidek, K., Wang, W., 1998. U/Pb zircon geochronologyand tempo of the end-Permian mass extinction. Science 280, 1039–1045.

Brewer, R., 1976. Fabric and Mineral Analysis of Soils. Krieger, New York. 482 p.

Buffett, B., Archer, D., 2004. Global inventory of methane clathrate: sensitivity to changes in the deep ocean. Earth and Planetary Science Letters 227, 185–199.

Coates, D.A., Stricker, G.D., Landis, E.R., 1990. Coal geology, coal quality and coal resources in Permian rocks of the Beacon Supergroup, Transantarctic Mountains, Antarctica. In: Splettstoesser, J.F., Dreschoff, G.A.M. (Eds.), Mineral Resource Potential of Antarctica, Antarctic Research Series. American Geophysical Union, vol. 51, pp. 133–162.

Colbert, E.H., 1974. *Lystrosaurus* from Antarctica. American Museum Novitates 2552 44 pp.

Colbert, E.H., 1983. Triassic vertebrates in the Transantarctic Mountains. In: Turner, M.D., Spletstoesser, J.F. (Eds.), Geology of the Central Transantarctic Mountains, Antarctic Research Series. American Geophysical Union, vol. 36, pp. 11–35.

Collinson, J.W., Elliot, D.H., 1984a. Geology of Coalsack Bluff, Antarctica. In: Turner, M.D., Splettstoesser, J.F. (Eds.), Antarctic Research Series, American Geophysical Union, vol. 36, pp. 97–102.

Collinson, J.W., Elliot, D.H., 1984b. Triassic stratigraphy of the Shackleton Glacier Area. In: Turner, M.D., Splettstoesser, J.F. (Eds.), Geology of the Central Transantarctic Mountains. Antarctic Research Series, American Geophysical Union, vol. 36, pp. 103–117.

Collinson, J.W., Isbell, J.I., Elliot, J.H., Miller, M.F., Miller, J.M.G., Veevers, J.J., 1994. Permian–triassic transantarctic basin. In: Veevers, J.J., Powell, C.M. (Eds.), Permian–Triassic Pangean Basins and Foldbelts along the Panthalassan Margin of Gondwanaland. Geological Society of America Memoir, vol. 184, pp. 173–222.

Collinson, J.W., Hammer, W.R., Askin, R.A., Elliot, D.H., 2006. Permian–Triassic boundary in the central Transantarctic Mountains Antarctica. Geological Society of America Bulletin 118, 747–763.

Czamanske, G.K., Wooden, J.L., Walker, R.J., Fedorenko, V.A., Simonov, O.N., Budahn, J.R., Siems, D.F., 2002. Geochemical, isotopic, and SHRIMP age data for Precambrian basement rocks, Permian volcanic rocks, and sedimentary host rocks to the ore-bearing intrusions, Noril'sk-Talnakh District, Siberian Russia. In: Ernst, W.G. (Ed.), Frontiers in Geochemistry; Konrad Krauskopf Volume; Global Inorganic Geochemistry. Geological Society of America, Boulder, pp. 238–270.

de Wit, M.J., Ghosh, J.G., de Villiers, S., Rakotosolofo, N., Alexander, J., Tripathi, A., Looy, C., 2002. Multiple organic carbon isotope reversals across the Permo–Triassic boundary of terrestrial Gondwanan sequences: clues to extinction patterns and delayed ecosystem recovery. Journal of Geology 110, 227–240.

Dickens, G.R., 2001. On the fate of past gas: what happens to methane released from a bacterially mediated gas hydrate capacitor? Geochemistry, Geophysics, Geosystems 2, doi:10.1029/200GC000131.

Dickens, G.R., O'Neil, J.R., Rea, D.K., Owen, R.M., 1995. Dissociation of oceanic methane hydrate as a cause of the carbon

isotopic excursion at the end of the Paleocene. Paleoceanography 10, 965–971.
Dickens, G.R., Castillo, M.M., Walker, J.C.G., 1997. A blast of gas in the latest Paleocene: simulating first-order effects of massive dissociation of oceanic methane hydrate. Geology 25, 259–262.
Elliot, D.H., 2000. Stratigraphy of Jurassic Pyroclastic Rocks in the Transantarctic Mountains. In: Storey, B.C., de Wit, M.T., Anderson, S.M., Anderson, H.M. (Eds.), Gondwana 10: Event Stratigraphy of Gondwana, vol. 2. Pergamon, Oxford, pp. 77–89.
Elliot, D.H., Hanson, R.E., 2001. Origin of widespread and exceptionally thick basaltic phreatomagmatic tuff breccia in the middle Jurassic Prebble and Mawson Formations Antarctica. Journal of Volcanology and Geothermal Research 111, 183–201.
Engoren, M., Retallack, G.J., 2004. Vertebrate extinction across the Permian–Triassic boundary in the Karoo Basin, South Africa: comment and reply. Geological Society of America Bulletin 116, 1293–1296.
Farabee, M.J., Taylor, E.L., Taylor, T.N., 1991. Late Permian palynomorphs from the Buckley Formation, central Transantarctic Mountains Antarctica. Review Palaeobotany Palynology 69, 353–368.
Farley, K.A., Mukhopadhyay, S., 2001. An extraterrestrial impact at the Permian–Triassic boundary? Science 293, U1–U3.
Food and Agriculture Organization, 1974. Soil Map of the World. Volume I, Legend. U.N.E.S.C.O., Paris. 59 p.
Food and Agriculture Organization, 1978a. Soil Map of the World. Volume VIII, North and Central Asia. U.N.E.S.C.O., Paris. 165 p.
Food and Agriculture Organization, 1978b. Soil Map of the World. Volume IX, Australasia. U.N.E.S.C.O., Paris. 221 p.
Food and Agriculture Organization, 1981. Soil Map of the World. Volume V, Europe. U.N.E.S.C.O., Paris. 199 p.
Foster, C.B., 1982. Spore-pollen assemblages of the Bowen Basin, Queensland (Australia): their relationship to the Permian–Triassic boundary. Review of Palaeobotany and Palynology 36, 165–183.
Foster, C.B., Stephenson, M.H., Marshall, C., Logan, G.A., Greenwood, P.F., 2002. A revision of *Reduviasporites* Wilson 1962: description, illustration, comparison and biological affinities. Palynology 26, 35–58.
Fricke, H.C., Clyde, W.C., O'Neil, J.R., Gingerich, P.D., 1998. Evidence for rapid climate change in North America during the Latest Paleocene thermal maximum: oxygen isotope compositions of biogenic phosphate from the Bighorn Basin (Wyoming). Earth and Planetary Science Letters 160, 193–208.
Gabet, E.J., 2003. Sediment transported by dry ravel. Journal of Geophysical Research 108 (1), doi:10.1029/20DIJB001686, 8 pp.
Gorter, J.D., 1996. Speculation on the origin of the Bedout High — a large circular structure of pre-Mesozoic age in the offshore Canning Basin, Western Australia. Petroleum Exploration Society of Australia News for 1996 (4), 32–33.
Grady, M.W., Wright, J.P., Carr, L.P., Pillinger, C.J., 1986. Compositional differences in enstatite chondrites based on carbon and nitrogen stable isotope measurements. Geochimica Cosmochimica Acta 50, 2799–2813.
Grice, K., Cao, S.Q., Love, G.D., Böttcher, M.E., Twitchett, R.J., Grosjean, E., Summons, R.E., Turgeon, S.C., Dunning, W., Jin, Y.G., 2005. Photic zone euxinia during the Permian–Triassic superanoxic event. Science 307, 706–709.
Gunner, J.D., 1983. Basement geology of the Beardmore Glacier Region. In: Turner, M.D., Splettstoesser, J.F. (Eds.), Geology of the Central Transantarctic Mountains. Antarctic Research Series, American Geophysical Union, vol. 36, pp. 1–9.
Hallam, A., Wignall, P.B., 1997. Mass Extinctions and their Aftermath. Oxford University Press, New York. 320 pp.
Hammer, W.R., 1990. Triassic terrestrial vertebrate faunas of Antarctica. In: Taylor, T.N., Taylor, E.L. (Eds.), Antarctic Paleobiology. Springer, Berlin, pp. 42–50.
Hammer, W.R., 1995. New therapsids from the upper Fremouw Formation (Triassic) of Antarctica. Journal of Vertebrate Paleontology 15, 105–112.
Hammer, W.R., Hickerson, W.J., 1994. A crested dinosaur from Antarctica. Science 264, 828–830.
Hesselbo, S.P., Grõcke, D.R., Jenkyns, H.C., Bjerrum, C.J., Farrimond, P., Bell, H.S.M., Green, O.R., 2000. Massive dissociation of gas hydrate during a Jurassic oceanic anoxic event. Nature 406, 392–395.
Heydari, E., Hassanzadeh, J., 2003. Deev Jahi model of the Permian–Triassic boundary mass extinction: a case for gas hydrates as the main cause of biological crisis on Earth. Sedimentary Geology 163, 147–163.
Holser, W.T., Schönlaub, H.P., Attrep Jr., M., Boeckelmann, K., Klein, P., Magaritz, M., Orth, C.J., Fenninger, A., Jenney, C., Kralik, M., Mauritsch, H., Pak, E., Schramm, J.M., Stattegger, K., Schmöller, R., 1989. A unique geochemical record at the Permian/Triassic boundary. Nature 337, 39–44.
Hooker, J.J., 1996. Mammalian biostratigraphy across the Paleocene–Eocene boundary in the Paris, London, and Belgian Basins. In: Knox, R.W.O., Corfield, R.M., Dunay, R.E. (Eds.), Correlations of the Early Paleogene in Northwest Europe. Geological Society of London Special Publication, vol. 101, pp. 205–218.
Horner, T.C., Krissek, L.A., 1991. Contributions of sedimentologic thermal alteration and organic carbon data to paleoenvironmental interpretation of fine-grained Permian clastics from the Beardmore Glacier region, Antarctica. In: Elliot, D.H. (Ed.), Contributions to Antarctic Research. Antarctic Research Series, American Geophysical Union, vol. 53, pp. 33–65.
Huey, R.B., Ward, P.D., 2005. Hypoxia, global warming and terrestrial Late Permian extinctions. Science 308, 398–401.
Huggett, R., Hesselbo, S., Sheldon, N.D., Retallack, G.J., 2003. Low oxygen levels in earliest Triassic soils: comment and reply. Geology 31, e20–e21.
Isbell, J.I., Cuneo, N.R., 1996. Depositional framework on Permian coal-bearing strata, southern Victoria land. Palaeogeography, Palaeoclimatology, Palaeoecology 125, 217–238.
Isbell, J.I., Askin, R.A., Retallack, G.J., 1999. Search for evidence of impact at the Permian–Triassic boundary in Antarctica and Australia — comment and reply. Geology 27, 859–860.
Isozaki, Y., 1997. Permian–Triassic boundary superanoxia and stratified superocean: records from the lost deep sea. Science 276, 235–238.
Izett, G.A., 1990. The Cretaceous/Tertiary boundary interval, Raton Basin, Colorado and New Mexico, and its content of shock-metamorphosed minerals: evidence relevant to the K/T boundary impact theory. Special Paper Geological Society of America 247 100 p.
Jahren, A.H., 2002. The biogeochemical consequences of the mid-Cretaceous superplume. Journal of Geodynamics 34, 177–191.
Jahren, A.H., Arens, N.C., Sarmiento, G., Guerrero, J., Amundson, R., 2001. Terrestrial record of methane hydrate dissociation in the Early Cretaceous. Geology 29, 159–162.
Jenkyns, H.C., 2003. Evidence for rapid climate change in the Mesozoic–Palaeogene greenhouse world. Royal Society of London Philosophical Transactions A361, 1885–1916.
Jessberger, E.K., 1999. Rocky cometary particulates: their elemental, isotopic and mineralogical ingredients. Space Science Reviews 90, 91–97.

Jin, Y.G., Wang, Y., Wang, W., Shang, Q.H., Cao, C.Q., Erwin, D.H., 2000. Pattern of marine mass extinction near the Permian–Triassic boundary in South China. Science 289, 432–436.
Kaiho, K., Kajiwara, Y., Nakano, T., Miura, Y., Kawahata, H., Tazaki, K., Ueshima, M., Chen, Z.-Q., Shi, G.R., 2001. End-Permian catastrophe by a bolide impact; evidence of a gigantic release of sulfur from the mantle. Geology 29, 815–818.
Kajiwara, Y., Yamakita, S., Ishida, K., Ishiga, H., Imai, A., 1994. Development of a largely anoxic stratified ocean and its temporary massive mixing at the Permian–Triassic boundary supported by the sulfur isotopic record. Palaeogeography, Palaeoclimatology, Palaeoecology 111, 367–379.
Kakuwa, Y., 1996. Permian–Triassic mass extinction event recorded in bedded chert sequence, southwest Japan. Palaeogeography, Palaeoclimatology, Palaeoecology 121, 35–51.
Katz, M.E., Cramer, B.S., Mountain, G.S., Katz, S., Miller, K.G., 2001. Uncorking the bottle: what triggered the Paleocene/Eocene methane release? Paleoceanography 16, 549–572.
Kent, D.V., Cramer, B.S., Lance, L., Wang, D., Wright, J.D., Van der Voo, R., 2003. A case for comet impact trigger for the Paleocene/Eocene thermal maximum and carbon isotope excursion. Earth Planetary Science Letters 211, 13–26.
Kent, D.V., Cramer, B.S., Lance, L., Wang, D., Wright, J.D., Van der Voo, R., 2004. A case for comet impact trigger for the Paleocene/Eocene thermal maximum and carbon isotope excursion. Earth Planetary Science Letters 217, 201–205.
Kennett, J.P., Stott, L.D., 1991. Abrupt deep sea warming, paleoceanographic changes and benthic extinctions at the end of the Palaeocene. Nature 353, 319–322.
Kerrick, D.M., 2001. Present and past non-anthropogenic CO_2 degassing from the solid Earth. Reviews of Geophysics 39, 565–585.
Khalil, M.A.K. (Ed.), 2000. Atmospheric Methane. Springer, Berlin. 351 pp.
Kidder, D.L., Worsely, T.R., 2004. Causes and consequences of extreme Permo–Triassic warming to globaly equable climate and relation to the Permo–Triassic extinction and recovery. Palaeogeography, Palaeoclimatology, Palaeoecology 203, 207–237.
Knoll, A.H., Bambach, R.K., Canfield, D.E., Grotzinger, J.P., 1996. Comparative earth history and the Late Permian mass extinction. Science 273, 452–457.
Koch, P.L., Zachos, J.C., Gingerich, P.D., 1992. Correlation between isotope records in marine and continental carbon reservoirs near the Palaeocene/Eocene boundary. Nature 358, 319–322.
Koch, P.L., Zachos, J.C., Dettman, D.L., 1995. Stable isotope stratigraphy and paleoclimatology of the Paleogene Bighorn Basin. Palaeogeography, Palaeoclimatology, Palaeoecology 115, 61–89.
Koeberl, C., Farley, K.A., Peucker-Ehrenbrink, B., Sephton, M.A., 2004. Geochemistry of the end-Permian extinction event in Austria and Italy: no evidence for an extraterrestrial component. Geology 32, 1053–1056.
Krull, E.S., 1998. Late Triassic hummocky coals near Schroeder Hill, central Transantarctic Mountains Antarctica. Antarctic Journal of the United States 31 (5), 35–37.
Krull, E.S., 1999. Permian palsa mires as paleonvironmental proxies. Palaios 14, 530–544.
Krull, E.S., Retallack, G.J., 2000. $\delta^{13}C$ depth profiles from paleosols across the Permian–Triassic boundary in Antarctica: evidence for methane release. Geological Society of America Bulletin 112, 1459–1472.
Krull, E.S., Retallack, G.J., Campbell, H.J., Lyon, G.L., 2000. $\delta^{13}C_{org}$ chemostratigraphy of the Permian–Triassic boundary in the Maitai Group, New Zealand: evidence for high latitude methane release. New Zealand Journal of Geology and Geophysics 43, 21–32.
Krull, E.S., Lehrmann, D.J., Druke, D.J., Kessel, B., Yu, Y.-Y., Li, R.-X., 2004. Stable carbon isotope stratigraphy across the Permian–Triassic boundary in shallow marine platforms, Nanpanjiang Basin, south China. Palaeogeography, Palaeoclimatology, Palaeoecology 204, 297–315.
Kump, L.R., Pavlov, A., Arthur, M.A., 2005. Massive release of hydrogen sulfide to the surface ocean and atmosphere during intervals of oceanic anoxia. Geology 33, 397–400.
Kvenvolden, K.A., 2000. Natural gas hydrate: introduction and history of discovery. In: Max, M.D. (Ed.), Natural Gas Hydrate in Oceanic and Permafrost Environments. Kluwer, Dordrecht, pp. 9–16.
Langenhorst, F., Kyte, F.T., Retallack, G.J., 2005. Re-examination of quartz grains from the Permian–Triassic boundary section at Graphite Peak Antarctica. Abstracts Lunar and Planetary Conference 2358.
Lucas, S.G., 1998. Global Triassic tetrapod biostratigraphy and biochronology. Palaeogeography, Palaeoclimatology, Palaeoecology 143, 347–384.
Maruoka, T., Koeberl, C., Hancox, P.J., Reimold, W.U., 2003. Sulfur geochemistry across a terrestrial Permian–Triassic boundary section in the Karoo Basin South Africa. Earth and Planetary Science Letters 206, 101–117.
McCarville, P., Crossey, L.J., 1996. Post-impact hydrothermal alteration of the Manson Impact Structure. In: Koeberl, C., Anderson, R.R. (Eds.), The Manson Impact Structure, Iowa: anatomy of an impact crater. Geological Society of America Special paper, vol. 302, pp. 347–376.
McElwain, J.C., 2005. Changes in carbon dioxide during oceanic anoxic event linked to intrusion into Gondwana coals. Nature 435, 479–482.
McLoughlin, S., Lindström, S., Drinnan, A.N., 1997. Gondwanan floristic and sedimentological trends during the Permian–Triassic transition: new evidence from the Amery Group, northern Prince Charles Mountains East Antarctica. Antarctic Science 9, 281–298.
McManus, H.A., Taylor, E.L., Taylor, T.N., Collinson, J.W., 2002. A petrified *Glossopteris* flora from Collinson Ridge, central Transantarctic Mountains: Late Permian or Early Triassic? Review of Palaeobotany and Palynology 120, 233–246.
Messenger, S., 2000. Identification of molecular cloud material in interplanetary dust particles. Nature 404, 968–971.
Michaelson, P., 2002. Mass extinction of peat-forming plants and the effect on fluvial styles caross the Permian–Triassic boundary, northern Bowen Basin Australia. Palaeogeography, Palaeoclimatology, Palaeoecology 179, 173–184.
Milkov, A., 2004. Global estimates of hydrate-bound gas in marine sediments: how much is really out there? Earth Science Reviews 66, 183–197.
Minagawa, M., Winter, D.A., Kaplan, I.R., 1984. Comparison of Kjehldahl and combustion tube methods for measurements of nitrogen isotope ratios in organic matter. Analytical Chemistry 56, 1859–1861.
Morante, R., 1996. Permian and early Triassic isotopic records of carbon and strontium in Australia and a scenario of events about the Permian–Triassic boundary. Historical Biology 11, 289–310.
Müller, M.J., 1982. Selected Climatic Data for a Global Set of Standard Stations for Vegetation Science. Junk, Hague. 306 pp.
Mundil, R., Metcalfe, I., Ludwig, K.R., Renne, P.R., Oberli, F., Nicoll, R.S., 2001. Timing of the Permian–Triassic biotic crisis; implications from new zircon U/Pb age data (and their limitations). Earth and Planetary Science Letters 187, 131–145.

Newton, R.J., Pevitt, E.L., Wignall, P.B., Bottrell, S.H., 2004. Large shifts in the isotopic composition of seawater sulfate across the Permian–Triassic boundary in northern Italy. Earth Planetary Science Letters 218, 331–345.

Nash, D.J., Smith, R.F., 2003. Properties and development of channel calcretes in a mountain catchment, Tabernas basin, southeast Spain. Geomorphology 50, 227–250.

Nisbet, E.G., 2002. Have sudden large releases of methane from geological reservoirs occurred since the last glacial maximum, and could such releases occur again? Royal Society of London Philosophical Transanctions A360, 581–607.

Norris, R.D., Rohl, U., 1999. Carbon cycling and chronology of climate warming during the Palaeocene/Eocene transition. Nature 401, 775–778.

Oddone, M., Vannucci, R., 1988. PGE and REE geochemistry at the B–W boundary in the Carnic and Dolomite Alps (Italy). Memoire Societa Geologica Italiana 34, 129–139.

Payne, J.L., Lehrmann, D.J., Wei, J.-Y., Orchard, M.J., Schrag, D.P., Knoll, A.H., 2004. Large perturbations of the carbon cycle during recovery from the end-Permian extinctions. Science 305, 506–509.

Pillinger, C.T., 1987. Stable isotope measurements of meteorites and cosmic dust grains. Royal Society of London Philosophical Transactions A323, 313–332.

Poreda, R.J., Becker, L., 2003. Fullerenes and interplanetary dust at the Permian–Triassic boundary. Astrobiology 3, 75–90.

Ravizza, G., Norris, R.N., Blusztajn, J., Aubry, M.-P., 2001. An osmium-isotope excursion associated with the late Paleocene thermal maximum: evidence of intensified chemical weathering. Paleoceanography 16, 155–163.

Reguera, J.L.C., 1998. Las melanges de Sierra del Rosario, Cuba occidental: tipos e importancia regionale. Mineria y Geologia 15, 3–9.

Reichow, M.K., Saunders, A.D., White, R.V., Prongle, M.S., Al Mukhamedov, A.I., Medvedev, A.I., Kirda, N.P., 2002. $^{40}Ar/^{39}Ar$ dates from west Siberian basin: Siberian flood basalt doubled. Science 296, 1846–1849.

Renne, P.R., Zhang, Z.C., Richards, M.A., Black, M.T., Basu, A.R., 1995. Synchrony and causal relations between Permian–Triassic boundary crisis and Siberian flood volcanism. Science 269, 176–177.

Renne, P.R., Melosh, H.J., Farley, K.A., Reimold, W.U., Koeberl, C., Rampino, M.R., Kelly, S.P., Ivanov, B.A., 2004. Is Bedout an impact crater? Take 2. Science 306, 611–612.

Retallack, G.J., 1995. Permian–triassic life crisis on land. Science 267, 77–80.

Retallack, G.J., 1996. Early Triassic therapsid footprints from the Sydney Basin Australia. Alcheringa 20, 301–314.

Retallack, G.J., 1997a. A Colour Guide to Paleosols. John Wiley and Sons, Chichester. 175 pp.

Retallack, G.J., 1997b. Palaeosols in the upper Narrabeen Group of New South Wales as evidence of Early Triassic palaeoenvironments without exact modern analogues. Australian Journal of Earth Sciences 44, 185–201.

Retallack, G.J., 1997c. Earliest Triassic origin of *Isoetes* and quillwort evolutionary radiation. Journal of Paleontology 71, 500–521.

Retallack, G.J., 1999a. Post-apocalyptic greenhouse paleoclimate revealed by earliest Triassic paleosols in the Sydney Basin Australia. Geological Society of America Bulletin 111, 52–70.

Retallack, G.J., 1999b. Permafrost palaeoclimate of Permian palaeosols in the Gerringong volcanics of New South Wales. Australian Journal of Earth Sciences 46, 11–22.

Retallack, G.J., 2001a. A 300 million year record of atmospheric carbon dioxide from fossil plant cuticles. Nature 411, 287–290.

Retallack, G.J., 2001b. Soils of the PastSecond Edition. Blackwell, Oxford. 404 pp.

Retallack, G.J., 2002a. *Lepidopteris callipteroides* (Carpentier) comb. nov., an earliest Triassic seed fern of the Sydney basin, southeastern Australia. Alcheringa 26, 475–500.

Retallack, G.J., 2002b. Carbon dioxide and climate over the past 300 Myr. Royal Society of London Philosophical Transactions A360, 659–673.

Retallack, G.J., 2005a. Earliest Triassic claystone breccias and soil-erosion crisis. Journal of Sedimentary Research 75, 663–679.

Retallack, G.J., 2005b. Pedogenic carbonate proxies for amount and seasonality of precipitation in paleosols. Geology 33, 333–336.

Retallack, G.J., Dilcher, D.L., 1988. Reconstructions of selected seed ferns. Annals Missouri Botanical Garden 75, 1010–1057.

Retallack, G.J., Hammer, W.R., 1998. Paleoenvironment of the Triassic therapsid Lystrosaurus in the central Transantarctic Mountains Antarctica. Antarctic Journal of the United States 31 (2), 33–35.

Retallack, G.J., Krull, E.S., 1999. Landscape ecological shift at the Permian–Triassic boundary in Antarctica. Australian Journal of Earth Sciences 46, 786–812.

Retallack, G.J., Krull, E.S., 2006. Carbon isotopic evidence for terminal-Permian methane outbursts and their role in extinctions of animals, plants, coral reefs, and peat swamps. In: Greb, S., DiMichele, W. (Eds.), Wetlands through time. Geological Society of America Special Paper, vol. 299, pp. 747–763.

Retallack, G.J., Veevers, J.J., Morante, R., 1996. Global early Triassic coal gap between Late Permian extinction and Middle Triassic recovery of peat-forming plants. Geological Society of America Bulletin 108, 195–207.

Retallack, G.J., Seyedolali, A., Krull, E.S., Holser, W.T., Ambers, C.A., Kyte, F.T., 1998. Search for evidence of impact at the Permian–Triassic boundary in Antarctica and Australia. Geology 26, 979–982.

Retallack, G.J., Wynn, J.G., Benefit, B.R, McCrossin, M.J., 2002. Paleosols and paleoenvironments of the middle Miocene Maboko Formation, Kenya. Journal of Human Evolution 42, 659–703.

Retallack, G.J., Smith, R.M.H., Ward, P.D., 2003. Vertebrate extinction across the Permian–Triassic boundary in the Karoo Basin South Africa. Geological Society of America Bulletin 115, 1133–1152.

Retallack, G.J., Jahren, A.H., Sheldon, N.D., Chakrabarti, R., Metzger, C.A., Smith, R.M.H., 2005. The Permian–Triassic boundary in Antarctica. Antarctic Science 17, 241–253.

Ryskin, G., 2003. Methane-driven oceanic eruptions and mass extinctions. Geology 31, 741–744.

Sarkar, A., Yoshioka, H., Edihara, M., Naraoka, H., 2003. Geochemical and organic isotope studies across the continental Permo–Triassic boundary of the Raniganj Basin, eastern India. Palaeogeography, Palaeoclimatology, Palaeoecology 191, 1–14.

Schopf, J.M., 1976. Morphologic interpretation of fertile structures in glossopterid gymnosperms. Review Palaeobotany Palynology 21, 25–64.

Scotese, C.R., 1994. Early Triasic paleogeographic map. In: Klein, G.V. (Ed.), Pangea: Paleoclimate, Tectonics and Sedimentation during Accretion, Zenith and Breakup of a Supercontinent. Geological Society of America Special Paper, vol. 288, p. 7.

Scott, A.R., Kaiser, W.R., Ayers, W.B., 1978. Thermogenic and secondary biogenic gases, San Juan Basin, Colorado and New Mexico — implications for coalbed gas producibility. American Association of Petroleum Geologists Bulletin 78, 1186–1209.

Seward, A.C., 1914. Antarctic Fossil Plants. British Museum Natural History, London. 49 pp.

Sheldon, N.D., Retallack, G.J., 2002. Low oxygen levels in earliest Triassic soils. Geology 30, 919–922.

Sigurdsson, H., d'Hondt, S., Arthur, M.A., Bralower, T.J., Zachos, J.C., Van Fossen, M., Channell, J.E.T., 1991. Glass from the Cretaceous/Tertiary Boundary in Haiti. Nature 349, 482–487.

Smith, R.M.H., Ward, P.D., 2001. Pattern of vertebrate extinction across an event bed at the Permian–Triassic boundary in the Karoo Basin of South Africa. Geology 29, 1147–1150.

Soil Survey Staff, 1999. Keys to Soil Taxonomy. Pocahontas Press, Blacksburg, Virginia. 600 pp.

Stott, L.D., Sinha, A., Thiry, M., Aubry, M.-P., Berggren, W.A., 1996. The transfer of ^{12}C changes from the ocean to the terrestrial biosphere across the Paleocene/Eocene boundary: criteria for terrestrial-marine correlations. In: Knox, R.W.O., Corfield, R.M., Dunay, R.E. (Eds.), Correlations of the Early Paleogene in Northwest Europe. Geological Society of London Special Publication, vol. 101, pp. 381–399.

Stummer, E., 1936. Die interglazialen Seen von Salzburg. Verhandlungen der Geologischen Bundesanstalt Wien 4, 101–107.

Svensen, H., Planke, S., Malthe-Sørenson, A., Jamtveit, B., Mykjlebust, R., Rassmussen, E., den, T., Rey, S.S., 2004. Release of methane from a volcanic basin as a mechanism for initial Eocene warming. Nature 429, 542–545.

Swanston, D.N., Swanson, F.J., 1976. Timber-harvesting, mass erosion, and steepland forest geomorphology. In: Coates, D.R. (Ed.), Geomorphology and Engineering. Dowden, Hutchinson and Ross, Stroudsburg, Pennsylvania, pp. 199–221.

Tasch, P., 1978. Permian palynomorphs (Coalsack Bluff, Mt. Sirius, Mt Picciotto) and other studies. Antarctic Journal of the United States 13 (4), 19–20.

Taylor, E.L., Taylor, T.N., Cuneo, N.R., 1992. The present is not the key to the past: a polar forest from the Permian of Antarctica. Science 257, 1675–1677.

Thomas, E., Shackleton, N.J., 1996. The Paleocene–Eocene benthic foraminiferal extinction and stable isotope anomalies. In: Knox, R.W.O., Corfield, R.M., Dunay, R.E. (Eds.), Correlations of the Early Paleogene in Northwest Europe. Geological Society of London Special Publication, vol. 101, pp. 401–411.

Tichy, G., Klappacher, W., Knapczyk, H., 1985. Geologische Übersicht. Salzburger Höhlenbuch 4, 27–45.

Twitchett, R.J., Looy, C.V., Morante, R., Visscher, H., Wignall, P.B., 2001. Rapid and synchronous collapse of marine and terrestrial ecosystems during the end-Permian biotic crisis. Geology 29, 351–354.

Vavra, C.L., 1989. Mineral reactions and controls on zeolite–facies alteration in sandstone from the central Transantarctic Mountains. Journal of Sedimentary Petrology 59, 688–703.

Vavra, C.L., Stanley, K.O., Collinson, J.W., 1981. Provenance and alteration of Triassic Fremouw Formation, central Transantarctic Mountains. In: Cresswell, M.M., Vella, P. (Eds.), Gondwana Five. Balkema, Rotterdam, pp. 149–153.

Visscher, H., Brinkhuis, H., Dilcher, D.L., Elsick, W.C., Eshet, Y., Looy, C.V., Rampino, M.R., Traverse, A., 1996. The terminal Paleozoic fungal event: evidence of terrestrial ecosystem destabilization and collapse. National Academy of Sciences Proceedings, U.S.A. 93, 2155–2158.

Ward, P.D., Montgomery, D.R., Smith, R., 2000. Altered river morphology in South Africa related to the Permian–Triassic extinction. Science 289, 1740–1743.

Ward, P.D., Botha, J., Buick, R., De Kock, M.O., Erwin, D.H., Garrison, G.H., Kirschvink, J.L., Smith, R., 2005. Abrupt and gradual extinction among Late Permian land vertebrates in the Karoo Basin, South Africa. Science 307, 709–714.

Wignall, P.B., 2001. Large igneous provinces and mass extinctions. Earth Science Reviews 53, 1–33.

Wignall, P.B., Thomas, B., Willink, R., Watling, J., 2004. Is Bedout an impact crater? Take 1. Science 306, 609–610.

Wignall, P.B., Newton, R., Brookfield, M.E., 2005. Pyrite framboid evidence for oxygen-poor deposition during the Permian–Triassic crisis in Kashmir. Palaeogeography, Palaeoclimatology, Palaeoecology 216, 183–188.

Wing, S.L., 1998. Late Paleocene–early Eocene floral and climatic change in the Bighorn basin. In: Aubry, M.-P., Lucas, S.G., Berggren, W.A. (Eds.), Late Paleocene–Early Eocene Climatic and Biotic Events in the Marine and Terrestrial Records. Columbia University Press, New York, pp. 380–400.

Wynn, J.G., 2003. Towards a physically based model of CO_2-induced stomatal frequency response. New Phytologist 157, 391–398.

Xu, D.-Y., Yan, Z., 1993. Carbon isotope and iridium event markers near the Permian/Triassic boundary in the Meishan section, Zhejiang Province, China. Palaeogeography, Palaeoclimatology, Palaeoecology 102, 171–176.

Yuan, T., Hyndman, R.D., Spence, G.D., Desmons, B., 1996. Seismic velocity increase and deep-sea gas hydrate concentration above a bottom-simulating reflector on the northern Cascade continental slope. Journal of Geophysical Research 101, 13655–13672.

Zachos, J.C., Lohmann, K.C., Walker, J.C.G., Wise, S.W., 1993. Abrupt climate change and transient climates during the Palaeogene: a marine perspective. Journal of Geology 101, 191–213.